ACS OMEGA

Open Access

http://pubs.acs.org/journal/acsodf

Article

Enhanced Retention of Cd(II) by Exfoliated Bentonite and Its Methoxy Form: Steric and Energetic Studies

Mostafa R. Abukhadra,* Nourhan Nasser, Ahmed M. El-Sherbeeny, and Wail Al Zoubi*

Cite This: *ACS Omega* 2024, 9, 11534−11550

Read Online

ACCESS | Metrics & More | Article Recommendations | Supporting Information

ABSTRACT: Synergistic studies were conducted to evaluate the retention potentiality of exfoliating bentonite (EXBEN) as well as its methanol hybridization derivative (Mth/EXBEN) toward Cd(II) ions to be able to verify the effects of the transformation processes. The adsorption characteristics were established by considering the steric and energetic aspects of the implemented advanced equilibrium simulation, specifically the monolayer model with a single energy level. Throughout the full saturation states, the adsorption characteristics of Cd(II) increased substantially to 363.7 mg/g following the methanol hybridized treatment in comparison to EXBEN (293.2 mg/g) as well as raw bentonite (BEN) (187.3 mg/g). The steric analysis indicated a significant rise in the levels of the active sites following the exfoliation procedure [retention site density (N_m) = 162.96 mg/g] and the chemical modification with methanol [retention site density (N_m) = 157.1 mg/g]. These findings clarify the improvement in the potential of Mth/EXBEN to eliminate Cd(II). Furthermore, each open site of Mth/EXBEN has the capacity to bind approximately three ions of Cd(II) in a vertically aligned manner. The energetic investigations, encompassing the Gaussian energy (less than 8 kJ/mol) plus the adsorption energy (less than 40 kJ/mol), provide evidence of the physical sequestration of Cd(II). This process may involve the collaborative impacts of dipole binding forces (ranging from 2 to 29 kJ/mol) and hydrogen binding (less than 30 kJ/mol). The measurable thermodynamic functions, particularly entropy, internal energy, and free enthalpy, corroborate the exothermic and spontaneous nature of Cd(II) retention by Mth/EXBEN, as opposed to those by EXBEN and BE.

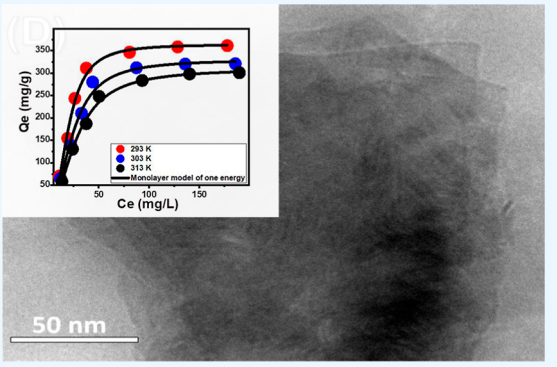

1. INTRODUCTION

Chemical pollution of water bodies, together with the ensuing negative consequences for people's wellness and environmental systems, are critical challenges that constitute an urgent risk to humanity's future well-being.[1,2] The main causes and contributing aspects to the current issue of polluted water supply and its related environmental side effects are the uncontrolled, broadly distributed, and continuous discharge of polluted effluents that result from mining, agriculture, and manufacturing activities.[3,4] The potential existence of hazardous metals within aquatic environments, whether in the form of soluble ions or chemical compounds bound to additional chemicals, displays a substantial threat to both the aquatic ecosystem and the health of humans.[3,5] The aforementioned chemicals have been categorized as highly toxic, nonbiodegradable, and carcinogenic agents with a propensity for bioaccumulation in humans as well as animal organisms.[6−8]

The presence of soluble heavy metals at concentrations greater than 0.05 mg/L has a malignant influence on the liver, lung, and kidneys by ingesting 1 L of polluted water every day.[9,10] Moreover, these metals demonstrate deleterious effects on the red blood cells, nervous system, and skin.[10,11] The frequent detection of Cd(II) contamination in water bodies can be primarily attributed to the disposal of effluents from various industrial activities, including smelting, cadmium−nickel battery fabrication, metal plating, pigment production, and alloy manufacturing.[4,12] The Cd(II) as soluble chemical ions has been categorized as a malignant and highly poisonous ion, necessitating its presence in water to be maintained at a level below about 0.003 mg/L.[13,14] Furthermore, the presence of Cd(II) contaminants has been found to result in several adverse health consequences, including acute disorders, pulmonary edema, itai−itai illness, chronic disorders, liver failure, emphysema, hypertension, osteomalacia, testicular atrophy, and kidney failure.[12,15] The inhibitory influence of Cd(II) ion on the leaf productivity of plants and seed germination, in addition to plant length and root elongation, has also been reported as having environmental side impacts.[16] Furthermore, the intrusion of elevated levels of Cd(II) has been found to have significant detrimental impacts on aquatic

Received: October 30, 2023
Revised: January 30, 2024
Accepted: February 13, 2024
Published: February 29, 2024

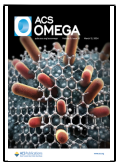

organisms and their ecosystems, as well as the commercial value of fish.[14,17]

Therefore, it is of the highest priority to address the issue of minimizing the level of Cd(II) within drinking water supplies given the established adverse effects on the natural environment and human health. Numerous investigations have advised the employment of both synthetic and natural adsorbents for adsorption-mediated elimination of soluble metal ions such as Cd(II). This approach is regarded as a simple, reliable, and cost-effective elimination method.[14,18,19] Nevertheless, the investigation of appropriate adsorbents remains a compelling area of study, implementing crucial criteria for selection including material accessibility, manufacturing expenses, recycling potential, adsorption capacity, equilibrium behavior, and kinetic rates.[7,20,21] The utilization of raw materials from nature as well as their modified varieties and hybrids for the elimination of metals has been recognized as the most efficient method of purification, considering some essential factors such as availability, affordability, scalability, and environmental concerns.[22,23]

Bentonite and related derivatives have received a great deal of attention as exceptionally efficient adsorbents.[24,25] Bentonite is a frequently employed geological term that refers to a kind of sedimentary rock that primarily consists of smectite clay minerals, specifically montmorillonite, along with other varieties of clay minerals. Additionally, it may contain other nonclay contaminants in its mineralogical composition.[26−28] Further investigation has been conducted to enhance the surface properties and physicochemical attributes of untreated bentonite, with a specific focus on its application as a possible adsorbent of both inorganic and organic molecules.[25,29,30] Various methods have been employed to modify or hybridize bentonite, including thermal treatment, alkaline modification, acid activation, metallic pillaring, metal oxide integration, scrubbing, polymer intercalation, and organic hybridizing using chemicals such as CTAB and starch.[25,29−31]

Recent studies have established methoxy-modified clay-based frameworks as advanced forms of tailored clay, exhibiting enhanced adsorption properties.[32,33] Through the utilization of environmentally friendly grafting techniques, the hydroxyl groups present on the innermost surface of natural clay can undergo intercalation by alcohol molecules that exist under ambient conditions.[33−35] Previous studies have focused on investigating the technical aspects of methoxy-kaolinite, but there is a dearth of research on the properties of methoxy-bentonite.[32,36] The strategy of methoxy-kaolinite synthesis necessitates a preliminary treatment phase to mitigate the influence of hydrogen bonding present within the crystalline structure of kaolinite. This entails the utilization of additional chemicals and a number of experimental approaches.[32,37] In contrast to kaolin, montmorillonite exhibits a higher level of hydroxyl layer interchangeability, enabling the insertion of alcohol molecules within its layered structure. This characteristic facilitates the binding of methanol with no need for extra pretreatment steps.[32,38] Therefore, it was hypothesized that the incorporation of methanol into bentonite-layered subunits would result in the formation of a multifunctional hybrid framework with enhanced physicochemical properties.[36] Moreover, during the past several decades, substantial advancements have been made in the field of the morphological transformation processes of clay, particularly in the area of separating or exfoliating the layered clay structures into discrete silicate sheets that possess two-dimensional geometrical structures.[39,40] The utilization of this approach has led to beneficial effects in the production of innovative nanostructures comprised of clay minerals, which demonstrate significant characteristics including considerable biological activity, adsorption potential, oxidation properties, surface reactivity, surface area, and dispersion properties.[38,41,42] Therefore, the formation of methoxy forms of the exfoliated bentonite nanosheets will result in highly promising adsorbents for a variety of soluble water pollutants.

Unfortunately, there has been a lack of sufficient implementation of thorough research on the properties of exfoliated bentonite, as well as its methoxy derivatives, as remarkably effective adsorbents for heavy metal ions. Therefore, the objective of this study is to assess the efficacy of synthesized exfoliated bentonite (EXBE) and methoxy exfoliated bentonite (Mth/EXBEN) in the retention of cadmium ions (Cd(II)), in contrast to that of raw bentonite. The experimental examinations were performed with particular emphasis on the Cd(II)/adsorbent interfaces. The accomplishment of this has been obtained based on the experimental findings and mathematical variables derived from advanced equilibrium approaches developed based on statistical physics theory involving both the steric and energetic aspects.

2. RESULTS AND DISCUSSION

2.1. Characterization of the Used Adsorbents. The X-ray diffraction (XRD) pattern of the bentonite specimen under investigation revealed an elevated content of montmorillonite, which was identified as the principal clay component. This was evident from the presence of distinctive peaks at about 6.55, 19.85, 25.10, and 28.35° (Figure 1A) (corresponding to cards

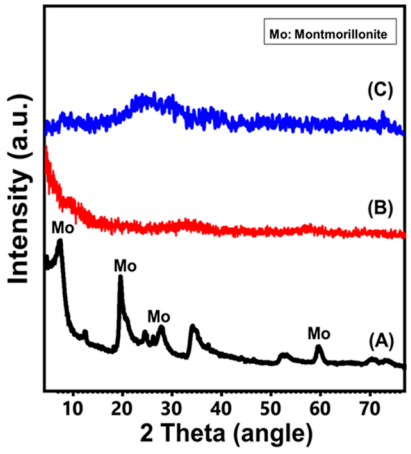

Figure 1. XRD patterns of bentonite (A), exfoliated bentonite (EXBEN) (B), and synthetic methoxy exfoliated bentonite (Mth/EXBEN) (C).

00-058-201 and no. 00-003-0010). Following the exfoliation activities, the patterns of the clay specimen appeared as a broad peak without substantial evidence supporting the presence of crystalline components (Figure 1B). The effective exfoliation as well as delamination of the investigated montmorillonite multilayered units was evidenced by their separation and the breakdown of the lattice structure given the amorphous materials (Figure 1C). The structural influence of methanol molecules upon the scrubbed bentonite sheets is not evident, and the resulting Mth/EXBEN product maintains its non-crystalline properties.

https://doi.org/10.1021/acsomega.3c08592
ACS Omega 2024, 9, 11534−11550

The bentonite particulates were detected in the scanning electron microscopy (SEM) photos as aggregated sheets that were densely packed on top of one another, resulting in the formation of clumps of agglomerated particles with massive outlines (Figure 2A). The noticeable tiny chunks observed

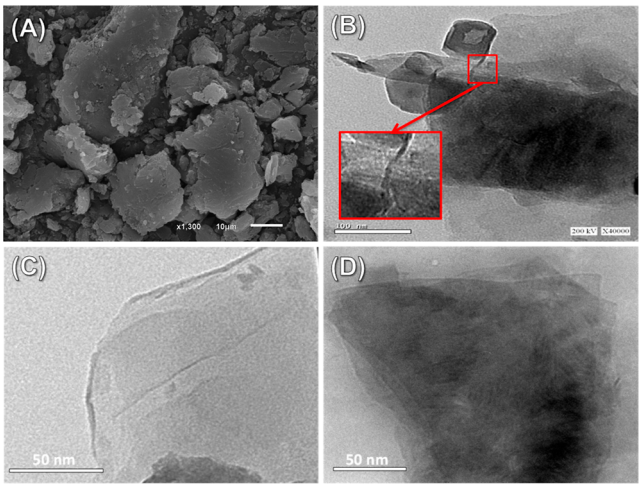

Figure 2. SEM of starting bentonite (A) and the HRTEM images of starting bentonite (B), EXBEN structure (C), and synthetic Mth/EXBEN structure (D).

across the exteriors of the bentonite plates might be attributed to the presence of mineral impurities instead of the different species of clay minerals (Figure 2A). The high-resolution transmission electron microscopy (HRTEM) photo clearly revealed the identifiable multilayered unit structures of montmorillonite, which is the basic constituent of bentonite (Figure 2B). The image depicted the characteristic multilayered configuration of the mineral, which is commonly referred to as the lattice finger structure (Figure 2B). Following the exfoliation operations, HRTEM photos of the bentonite revealed successful separation of the densely packed montmorillonite layers, resulting in the formation of distinct and isolated aluminosilicate sheets (Figure 2C). This process significantly enhanced the surface reactivity as well as improved the surface area. The HRTEM photos of the developed methoxy exfoliated bentonite (Mth/EXBEN) reveal the separation of the condensed, layered bentonite into distinct individual layers (Figure 2D). Additionally, the photos display irregular parts of dark gray, which can be attributed to the presence of functionalized alcohol molecules and their reaction with the surface of EXBEN (Figure 2D).

The exfoliating and alcohol modification result in a notable increase in the surface area, with values of 141.4 and 143.2 m^2/g observed for EXBEN and Mth/EXBEN, respectively, compared to the initial surface area of 91 m^2/g for bentonite (Table 1). Regarding the porosity, the modification processes resulted in a significant increase in the microporosity as compared to mesoporosity, which signifies the reduction in the interstitial pores between the BEN particles and the exposure of the structural pores of the silicate sheets or the common lenticular pores that relate to the cornflake structures of the exfoliated bentonite sheets (Table 1). The integration of methanol exhibits slight effect either of the surface area or the porosity properties of the EXBEN particles and this slight impact might be assigned to the dissolution of some of the existing organic impurities.

Table 1. Textural Properties of BEN, EXBEN, and Mth/EXBEN

sample	surface area (m^2/g)	micropores volume (cm^3/g)	mesopores volume (cm^3/g)	total volume (cm^3/g)	average pore diameter (nm)
BEN	91	0.013	0.262	0.312	10.4
EXBEN	141.4	0.246	0.143	0.389	4.6
Mth /EXBEN	143.2	0.248	0.144	0.392	4.3

The FT-IR spectra analysis revealed that the natural bentonite sample had prominent peaks corresponding to its specific functional groups, including structural OH, intercalated water molecules, structural Si−O, and functional Al−O (Figure 3A). These functional groups were identified by

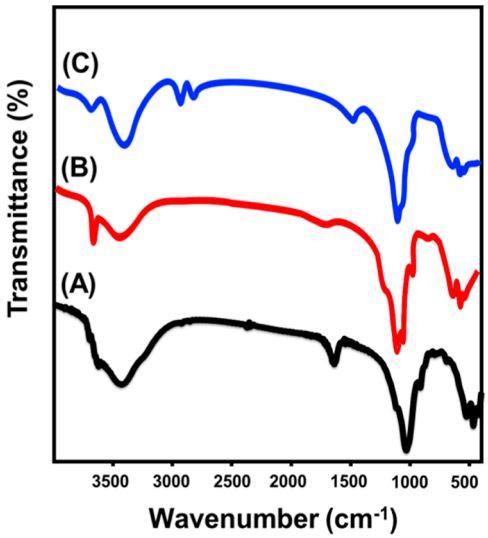

Figure 3. FT-IR spectra of bentonite (A), synthetic EXBEN structure (B), and synthetic Mth/EXBEN (C).

absorption bands noticed at wavenumbers of 3400, 1640, 1000.2, and 918.3 cm^{-1}, respectively (Figure 3A).[25,26] Furthermore, the discernible attenuated peaks within the spectral region spanning roughly 400 to 1000 cm^{-1} may be attributed to the characteristic bands associated with Si−O−Al and Si−O−Mg in addition to Mg−Fe−OH (Figure 3A).[26,43] The spectra of EXBEN exhibit absorbance bands that are similar to those reported in unprocessed bentonite but with notable differences in their precise locations, reduced intensities, and the disappearance of smaller bands (Figure 3B). This illustrates the possible destruction of the functional alumina octahedron and silica tetrahedron units of starting bentonite, as well as the efficient dispersion of these units into discrete or singular sheets.[40,44] Upon treatment of EXBEN with methanol, the resulting FT-IR spectrum reveals a reduction in the intensity of the characteristic bands associated with the inner surface-hydroxyl-bearing functioning groups. This demonstrates the interaction effect of the Al−OH chemical groups within the bentonite multilayered units through the alcohol modification process (Figure 3C).[32,33] Meanwhile, the observed bands at 2951 and 2860 cm^{-1} can be attributed to the bending vibrations of the methanol chemical groups that have been grafted onto the sample (Figure 3C).[33,35] The aforementioned findings, together with the

https://doi.org/10.1021/acsomega.3c08592
ACS Omega 2024, 9, 11534−11550

evident displacement of the respective bands associated with the aluminosilicate chemical and structural groups that construct various layers of bentonite, indicate the effective interaction between the EXBEN reactive groups and the alcohol molecules, resulting in the development of a methoxy-modified form of exfoliating bentonite (Mth/EXBEN).

2.2. Adsorption Studies. *2.2.1. Effect of pH.* The current investigation analyzes the influence of pH values spanning 2 to 7 on the adsorption capacity of Cd(II) utilizing the three different adsorbents (BEN, EXBEN, and Mth/EXBEN). It was decided to set the maximum limit at pH 7 to prevent the potential formation of hydroxide species of Cd(II) as a precipitate at higher pH settings. All of the experiments mentioned earlier were completed with strict regulation of the key factors at specified values. These variables included a Cd(II) level of 100 mg/L, a solid dosage of 0.2 g/L, a volume of 100 mL, a temperature of 20 °C, and a period of 60 min. The retention capacities of Cd(II) using BEN, EXBEN, and Mth/EXBEN show notable improvements as the pH of the impure solutions being tested increases from pH 2 (4.7 mg/g (BE), 10.3 mg/g (EXBEN), and 18.3 mg/g (Mth/EXBEN)) to pH 7 (58.6 mg/g (BEN), 77.2 mg/g (EXBEN), and 83.2 mg/g (Mth/EXBEN)) (Figure 4). Therefore, these materials

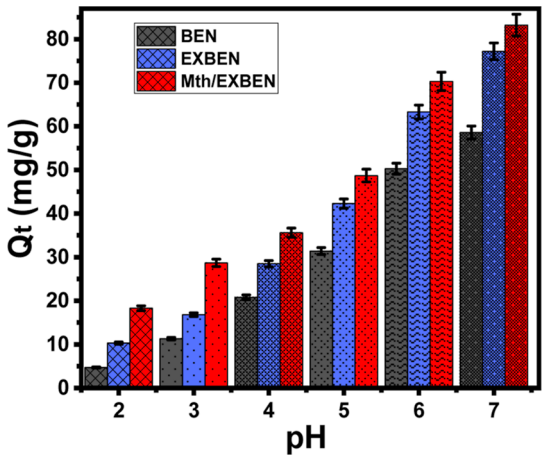

Figure 4. Influence of the pH on the retention of Cd(II) by BEN, EXBEN, and Mth/EXBEN.

have the potential to be used as effective adsorbents in the actual treatment procedures, aligning with the range of pH levels of 6 to 9, as advised by the US Environmental Protection Agency (EPA) for the purification of industrial effluents.[45] The presented behaviors demonstrate a significant association between the pH and the ionization properties of Cd(II) ions, in addition to the charges across the exterior surfaces of BEN, EXBEN, and Mth/EXBEN.[46] Cadmium occurs as positive cations (Cd^{2+}) throughout the pH range tested, and above pH 8, it forms hydroxide precipitates ($[Cd(H_2O_6)]^{2+}$). As alkaline levels of Cd(II) solutions expanded, the reactive functional groups of BEN, EXBEN, and Mth/EXBEN became more and more deprotonate, which resulted in their outer surfaces being totally submerged with negative charges.[47] The negatively charged outer interfaces of BEN, EXBEN, and Mth/EXBEN play a crucial role in facilitating the electrostatic interactions between Cd(II) and its positively charged state.[48]

2.3. Kinetic Studies. *2.3.1. Effect of Contact Time.* An investigation was conducted to examine the influence of the period of Cd(II) adsorption on the experimentally determined qualities of BEN, EXBEN, and Mth/EXBEN within a time range spanning from 20 to 300 min. This was achieved following the manipulation of other significant variables to predetermined values [Cd(II) concentration: 100 mg/L; pH: 7; volumes: 100 mL; temperature: 20 °C; solid material dosage: 0.2 g/L]. The considerable rise in the detected uptake rates, as well as the estimated quantities of retained Cd(II) in mg/g, demonstrate the enhancement in the effectiveness of BE, EXBEN, and Mth/EXBEN in terms of the expansion in the testing uptake duration (Figure 5A). Furthermore, it is worth noting that the duration of testing has a regulatory influence on the observed increments. The increased impact of Cd(II) retention activities using BE, EXBEN, and Mth/EXBEN can be easily noticed over a period of 120 min (BE) and 160 min (EXBEN and Mth/EXBEN) (Figure 5A). Following the designated duration of the interaction, there were no observable changes or enhancements in the retention rates of Cd(II) or the sequestrated quantities. This indicates that their uptake systems established a state of stability after these intervals, which was recognized as the point of adsorption equilibrium (Figure 5A). The measured Cd(II) equilibrium retention levels of the BE, EXBEN, and Mth/EXBEN particles were 112.7 (BEN), 131 (EXBEN), and 154.7 mg/g (Mth/EXBEN) (Figure 5A). The preliminary periods of the accomplished experiments indicated that the existence of numerous free and structurally reactive sites or sequestration receptors across the outermost surfaces of BE, EXBEN, and Mth/EXBEN resulted in significant enhancements with regard to the speed of Cd(II) uptake alongside the quantities of Cd(II) retained.[37] The prolonged time frame for testing led to a considerable reduction in the availability of the binding sites of BE, EXBEN, and Mth/EXBEN due to the continual retention of Cd(II) and subsequent occupancy of these sites, depleting their availabilities. As a result, following a predetermined time frame, the rates at which Cd(II) was absorbed displayed a notable decrease, and the retention properties of BE, EXBEN, and Mth/EXBEN remained unchanged or exhibited negligible improvement. The equilibrium states of BE, EXBEN, and Mth/EXBEN were successfully determined following the full occupancy of receptors or empty reaction sites by Cd(II).[3]

2.3.2. Intra-Particle Diffusion Behavior. Intraparticle diffusion curves can be used to describe how Cd(II) is taken up by BEN, EXBEN, and Mth/EXBEN. These curves display three particular segments that have various slopes. The curves obtained in the current study demonstrate a lack of observable crossings with the beginning points, suggesting the coexistence of various adsorption processes alongside Cd(II) diffusion pathways (Figure 5B).[46,49] The operational procedure consists of several essential stages.[50] These stages include: (A) the retention of Cd(II) through the receptors distributed on the exteriors of BEN, EXBEN, and Mth/EXBEN (external or boundary); (B) intraparticle diffusion; and (C) the operating reactions encompassing saturation alongside stability states. The first findings of this study suggest that the primary mechanisms involved in the experimental process were the external adsorption activities of Cd(II) (Figure 5B). The efficacy of the Cd(II) retention process during this phase relies on the total number of unfilled receptors on the surface of BEN, EXBEN, and Mth/EXBEN.[51] The identification of newly formed phases was enhanced by prolonging the time, showcasing the effectiveness of many additional processes known as layered adsorption approaches (Figure 5B).[17,50]

https://doi.org/10.1021/acsomega.3c08592
ACS Omega 2024, 9, 11534−11550

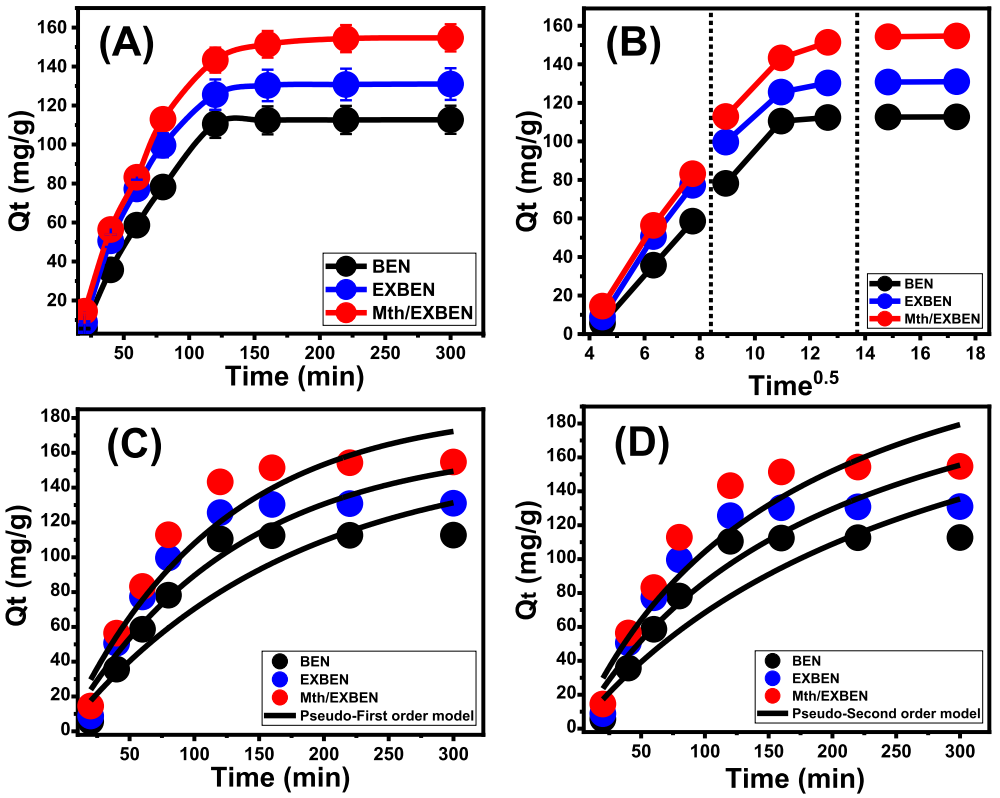

Figure 5. Influence of the contact time on the retention efficiencies of Cd(II) by BEN, EXBEN, and Mth/EXBEN (A), intraparticle diffusion curves for the retention of Cd(II) (B), fitting of the determined retention results with pseudo-first order model (C), and fitting of the determined retention results with pseudo-second order model (D).

Furthermore, these supplementary procedures additionally incorporate the influence of Cd(II) diffusion activities. It has been shown that the final three stages demonstrate a dominant presence whenever the equilibrium states of BEN, EXBEN, and Mth/EXBEN are attained (Figure 5B). This finding suggests that the interaction binding sites have been entirely filled by the Cd(II) ions that were effectively retained.[3,7] The elimination of Cd(II) during this stage is subject to several variables, such as molecular interactions and interionic attraction mechanistic pathways.[47]

2.3.3. Kinetic Modeling. The kinetic properties of Cd(II) retention operations using BEN, EXBEN, and Mth/EXBEN were explained using the standard kinetic assumptions of the pseudo-first-order (P.F.) and pseudo-second-order (P.S.) theoretical models. The level of agreement that existed between the Cd(II) retention processes and the kinetic concepts of the two distinct models has been examined through the use of defined nonlinear fitting parameters, as denoted by the corresponding equations and determined from the correlation coefficient (R^2) together with the Chi-squared (χ^2) information (Table 2 and Figure 5C,D). The established levels of R^2, alongside χ^2, suggest that the kinetic characteristics and suggestions of the P.F. model have a better correlation with the adsorption processes of Cd(II) using BEN, EXBEN, and Mth/EXBEN in comparison with the assessed P.S. model. The results gathered from the tests carried out on BE, EXBEN, and Mth/EXBEN under a state of equilibrium [112.7 mg/g (BEN), 131 mg/g (EXBEN), and 154.7 mg/g (Mth/EXBEN)] were observed to exhibit a high level of agreement with the results derived from computational calculations based on the P.F. model [121.6 mg/g (BEN), 143.3 mg/g (EXBEN), and 166.1 mg/g (Mth/EXBEN)]. This agreement provides further support for the previous results obtained in the kinetic analysis (Table 2). According to the basic assumptions of the

Table 2. Mathematical Parameters of the Studied Kinetic Models

material	model	parameters	values
BEN	pseudo-first-order	K_1 (1/min)	0.0058
		$Q_{e(Cal)}$ (mg/g)	121.6
		R^2	0.90
		χ^2	4.6
	pseudo-second-order	k_2 (mg/g min)	1.3×10^{-5}
		$Q_{e(Cal)}$ (mg/g)	265.5
		R^2	0.87
		χ^2	6.2
EXBEN	pseudo-first-order	K_1 (1/min)	0.99
		$Q_{e(Cal)}$ (mg/g)	143.3
		R^2	0.89
		χ^2	5.3
	pseudo-second-order	k_2 (mg/g min)	1.9×10^{-5}
		$Q_{e(Cal)}$ (mg/g)	158.6
		R^2	0.85
		χ^2	7.4
Mth/EXBEN	pseudo-first-order	K_1 (1/min)	0.0086
		$Q_{e(Cal)}$ (mg/g)	166.07
		R^2	0.93
		χ^2	3.4
	pseudo-second-order	k_2 (mg/g min)	2.1×10^{-5}
		$Q_{e(Cal)}$ (mg/g)	279.9
		R^2	0.91
		χ^2	5.3

https://doi.org/10.1021/acsomega.3c08592
ACS Omega 2024, 9, 11534−11550

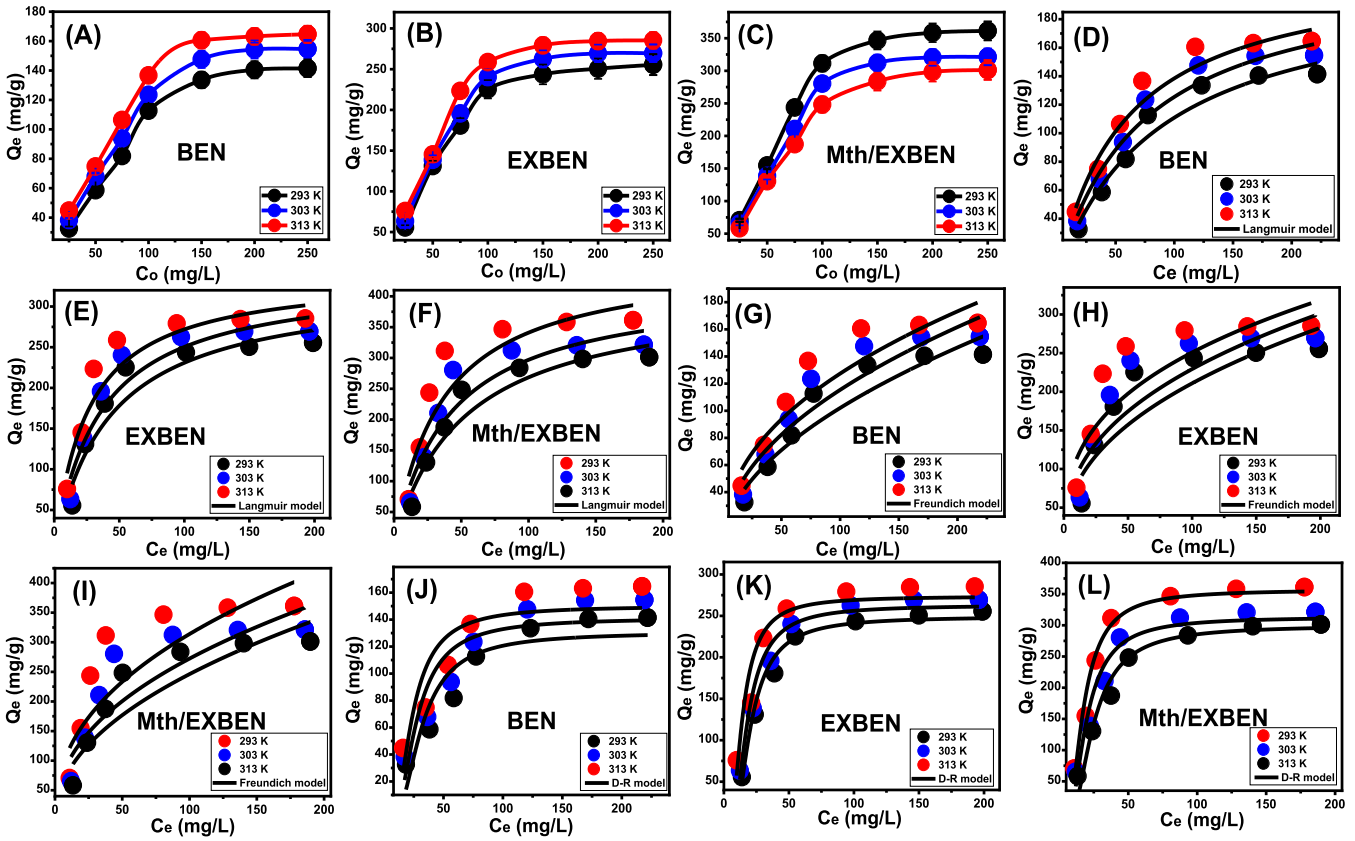

Figure 6. Influence of the Cd(II) concentration on the retention efficiencies of Cd(II) [(A) BEN, (B) EXBEN, and (C) Mth/EXBEN], fitting of the retention behaviors of Cd(II) with classic Langmuir isotherm [(D) BEN, (E) EXBEN, and (F) Mth/EXBEN], fitting of the retention behaviors of Cd(II) with classic Freundlich isotherm [(G) BEN, (H) EXBEN, and (I) Mth/EXBEN], and fitting of the retention behaviors of Cd(II) with classic D−R isotherm [(J) BEN, (K) EXBEN, and (L) Mth/EXBEN].

P.F. theory, it is proposed that the key factors impacting the retention of Cd(II) using BEN, EXBEN, and Mth/EXBEN were physical mechanisms, specifically the forces of van der Waals and/or electrostatic attractions.[52,53] Although the P.F. model's formula for elimination of Cd(II) by BEN, EXBEN, and Mth/EXBEN is verified to be better compatible compared to the presented equation of the P.S. model, the analyzed retention features still exhibit notable agreement with the proposed kinetics of the P.S. theory. Previous studies have demonstrated that various weak chemical effects, such as chemical-based complexing, hydrophobic bonds, hydrogen binding, and electron-based sharing, are likely to play a role in either enhancing or having minimal effects on the removal of Cd(II) by BEN, EXBEN, and Mth/EXBEN.[46,52] Following the formation of a chemically bound Cd(II) layer, a physically adsorbed Cd(II) layer was developed, using the previous layer as a basis.[54]

2.4. Equilibrium Studies. *2.4.1. Effect of Cd(II) Concentrations.* The impact of varying starting concentrations of Cd(II) was examined in order to determine the best capacities of BEN, EXBEN, and Mth/EXBEN, in addition to the corresponding equilibrium states, within the systematically determined range of 25−250 mg/L. The remaining retention factors have been chosen to be at predefined values [the dosage is set at 0.2 g/L, the duration is set at 24 h, the volume is set at 100 mL, the pH is set at pH 7; and the temperature tested from 293 to 313 K]. The quantities of Cd(II) that were retained using BEN, EXBEN, and Mth/EXBEN showed a significant increase when the concentrations of Cd(II) increased (Figure 6A−C). The increased concentrations of Cd(II) ions within a given volume led to a noticeable improvement in their transfer, migration, and driving forces, thereby promoting interaction as well as collision potential with a greater number of accessible and functional receptors situated on the exteriors of BEN, EXBEN, and Mth/EXBEN. As a result, the effectiveness of the Cd(II) adsorption activities carried out by BEN, EXBEN, and Mth/EXBEN significantly increased.[55] The observed levels of Cd(II) adsorption demonstrate a proportional rise in relation to the higher starting concentration until certain thresholds. Following this, an increase in the initial concentration of Cd(II) does not have a discernible impact on the amount of ions retained using BEN, EXBEN, and Mth/EXBEN. As a result, the equilibrium stages of these materials can be distinguished, allowing for the determination of their respective maximum adsorption capacities for Cd(II) ions. At concentrations exceeding 200 mg/L, equilibrium conditions established in the existence of BEN yield adsorption capacities of 141.6 mg/g (293 K), 154.7 mg/g (303 K), and 164.5 mg/g (313 K) (Figure 6A). The experimental results indicate that the equilibrium efficiencies of EXBEN, when subjected to a concentration of 200 mg/L Cd(II), are 255.8 mg/g at a temperature of 293 K, 269.6 mg/g at 303 K, and 285.4 mg/g at 313 K (Figure 6B). The equilibrium level of Cd(II) that corresponds to Mth/EXBEN will be assumed to be 200 mg/L. The relevant capacities at different temperatures are as follows: 361.3 mg/g at 293 K, 321.4 mg/g at 303 K, and 301.4 mg/g at 313 K (Figure 6C). The enhanced performance of EXBEN and Mth/EXBEN in

https://doi.org/10.1021/acsomega.3c08592
ACS Omega 2024, 9, 11534−11550

Table 3. Mathematical Parameters of the Studied Classic Isotherm Models

			293 K	303 K	313 K
BEN	Langmuir model	Q_{max} (mg/g)	207.7	216.05	218.8
		b (L/mg)	0.0114	0.0138	0.017
		R^2	0.974	0.979	0.975
		χ^2	0.79	0.65	0.76
	Freundlich model	$1/n$	0.52	0.48	0.44
		k_F (mg/g)	9.17	12.27	16.48
		R^2	0.92	0.92	0.91
		χ^2	2.28	2.3	2.5
	D−R model	β (mol^2/kJ^2)	0.022	0.014	0.011
		Q_m (mg/g)	130.6	141.16	150.12
		R^2	0.859	0.857	0.0.84
		χ^2	0.4	0.05	0.1
		E (kJ/mol)	4.76	5.97	6.74
EXBEN	Langmuir model	Q_{max} (mg/g)	328.06	337.9	341.2
		b (L/mg)	0.023	0.028	0.039
		R^2	0.92	0.93	0.94
		χ^2	4.26	3.6	3.16
	Freundlich model	$1/n$	0.42	0.4	0.34
		k_F (mg/g)	30	37.5	51.3
		R^2	0.83	0.83	0.82
		χ^2	10.02	9.97	9.7
	D−R model	β (mol^2/kJ^2)	0.012	0.011	0.0084
		Q_m (mg/g)	249.2	262.9	273.5
		R^2	0.98	0.97	0.93
		χ^2	0.73	1.25	3.47
		E (kJ/mol)	6.45	6.74	7.71
Mth/EXBEN	Langmuir model	Q_{max} (mg/g)	463.6	422.002	408.48
		b (L/mg)	0.027	0.023	0.019
		R^2	0.9	0.92	0.94
		χ^2	8.6	5.9	4.22
	Freundlich model	$1/n$	0.42	0.44	0.47
		k_F (mg/g)	43.6	35.5	27.3
		R^2	0.8	0.83	0.86
		χ^2	18.2	13.8	10.5
	D−R model	β (mol^2/kJ^2)	0.0095	0.011	0.018
		Q_m (mg/g)	356.8	313.25	299.5
		R^2	0.97	0.95	0.96
		χ^2	2.05	3.67	3.3
		E (kJ/mol)	7.25	6.74	5.27

the elimination of Cd(II) when compared to BE particles can be attributed to the significant improvement of surface area coupled with the reactivity properties of the separated aluminosilicate single layers. These layers possess semicrystalline attributes and an extensive number of chemically reactive sites, most notably the siloxane groups. Moreover, the methanol treatment steps result in the significant incorporation of additional active hydroxyl groups as effective uptake centers. The observed decrease in the adsorption effectiveness of Cd(II) by Mth/EXBEN with increasing temperature indicates that the mechanisms of adsorption are characterized by exothermic behavior in contrast to BE and EXBEN, which display endothermic behaviors, and their adsorption performances are enhanced with the testing temperature.

2.4.2. Giles's Classification. The criteria specified by Giles' categorization were used to classify the Cd(II) equilibrium curves employing BEN, EXBEN, and Mth/EXBEN. The analysis determined that the observed curves demonstrated an L-type state of equilibrium (Figure 6A−C). The equilibrium characteristics of the L-type demonstrate the significant impacts that arise from the intermolecular attraction interactions involved in the adsorption mechanisms of Cd(II) by BEN, EXBEN, and Mth/EXBEN. The aforementioned impacts are also enhanced by the powerful interactions that exist between Cd(II) ions and the chemically reacting structures of BEN, EXBEN, and Mth/EXBEN.[56] According to the characteristics of the L-type isotherm, it has been feasible to predict the complete formation of Cd(II) monolayers over the outer surfaces of BEN, EXBEN, and Mth/EXBEN particles.[57] Furthermore, the outlined isothermal pattern suggests the formation of BEN, EXBEN, and Mth/EXBEN particulates with diverse and substantial activated and free uptake sites. The binding sites exhibit notable affinity toward Cd(II) ions throughout the course of the adsorption procedure, particularly under conditions of low starting concentrations.

2.4.3. Classic Isotherm Models. This work investigates the adsorption behavior of Cd(II) on BEN, EXBEN, and Mth/EXBEN particulates under the equilibrium conditions. The Langmuir, Freundlich, and Dubinin−Radushkevich (D−R)

https://doi.org/10.1021/acsomega.3c08592
ACS Omega 2024, 9, 11534−11550

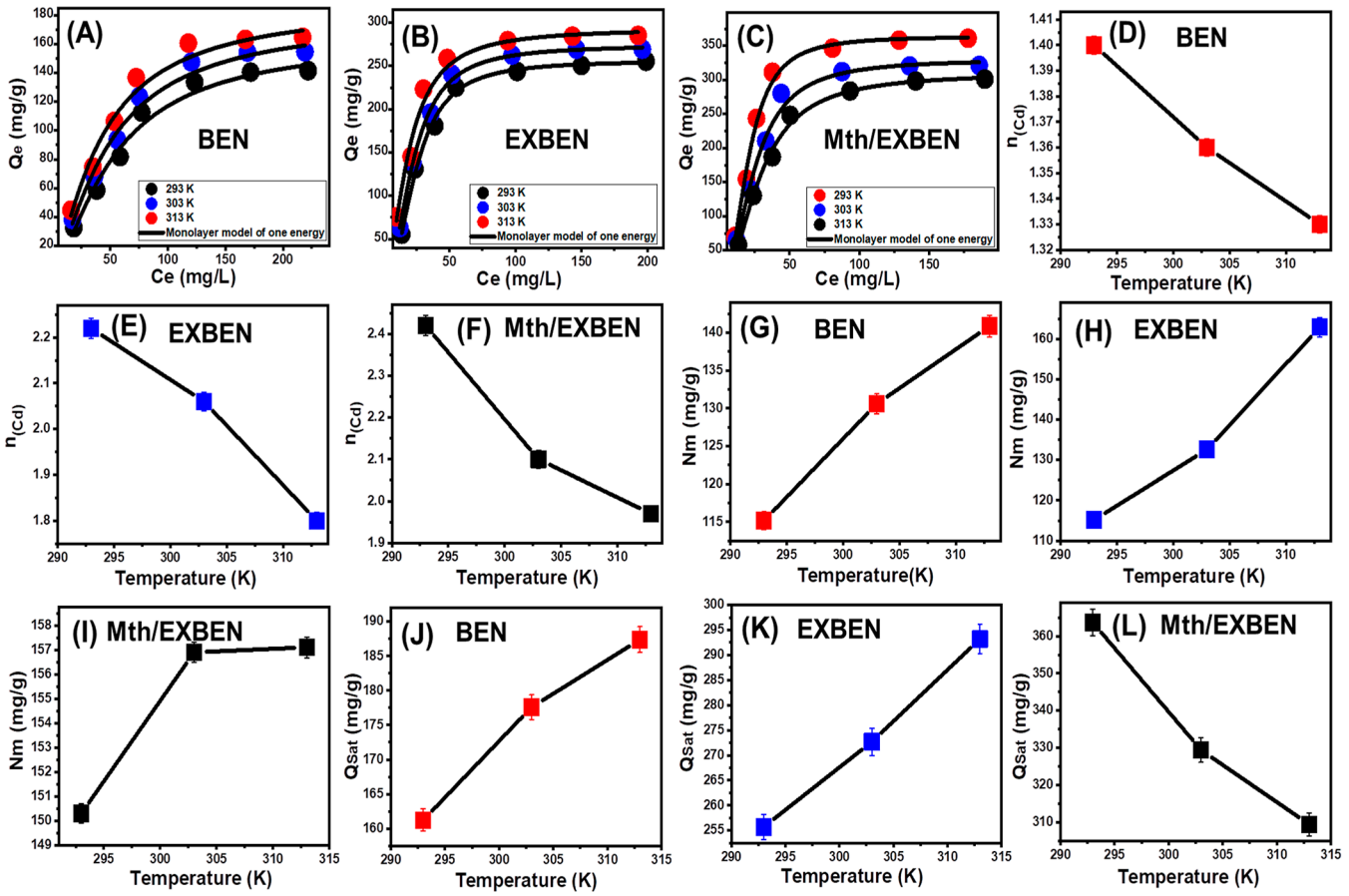

Figure 7. Fitting of the retention behaviors of Cd(II) with advanced Monolayer with single energy site isotherm [(A) BEN, (B) EXBEN, and (C) Mth/EXBEN], change in the number of adsorbed Cd(II) ion per single site [(D) BEN, (E) EXBEN, and (F) Mth/EXBEN], change in the occupying active sites density during the uptake of Cd(II) [(G) BEN, (H) EXBEN, and (I) Mth/EXBEN], and change in the saturation adsorption capacity with temperature [(J) BEN, (K) EXBEN, and (L) Mth/EXBEN].

isotherm hypotheses are employed to analyze the adsorption process. The level of concordance between the equilibrium hypotheses of each given model and the experimentally measured Cd(II) retention behaviors was evaluated using nonlinear regression analysis, employing the corresponding equations of the various models. The assessment was formulated based on the use of the correlation coefficient (R^2) and the Chi-squared (χ^2) quantities, as depicted in Table 3 and Figure 6D−L. The findings derived from the examination of R^2 and χ^2 demonstrate that the Cd(II) retention characteristics exhibited by BEN, EXBEN, and Mth/EXBEN particulates are in greater agreement with the principles of the Langmuir isotherm hypothesis (Table 3 and Figure 6D−F) as opposed to the underlying assumptions of the Freundlich hypothesis (Table.3 and Figure 6G−I). The Langmuir isotherm model is utilized to explain the homogeneous adsorption behavior of Cd(II) ions on the vacant and active binding positions of BEN, EXBEN, and Mth/EXBEN particulates in a monolayer configuration.[52,53] Moreover, the retention properties of BEN, EXBEN, and Mth/EXBEN particulates toward Cd(II) are characterized by RL values beneath 1, suggesting the favorable nature of these processes.[7,51] The postulated upper limit of adsorption capacity (Q_{max}) for Cd(II) by BEN at a variety of temperatures varies as follows: 207.7 mg/g (293 K), 216 mg/g (303 K), and 218.8 mg/g (313 K). The computed values obtained for EXBEN are 328 mg/g at a temperature of 293 K, 337.9 mg/g at 303 K, and 341.2 mg/g at 313 K. The assumed maximum capacities (Q_{max}) for the capture of Cd(II) by Mth/EXBEN at various temperatures are 463.2 mg/g at 293 K, 422 mg/g at 303 K, and 408.5 mg/g at 313 K (Table.3).

Regardless of whether the structure of the system is heterogeneous or homogeneous, the isotherm-based concepts of the D−R model (Figure 6J−L) provide an in-depth analysis of the energy differences exhibited by BEN, EXBEN, and Mth/EXBEN particulates across the course of Cd(II) retention. One of the most important derived parameters obtained from the D−R assessment findings is the Gaussian energy (E) that is employed to determine the particular Cd(II) uptake mechanisms (chemical or physical). Adsorption activities with E values beneath 8 kJ/mol, between 8 and 16 kJ/mol, and over 16 kJ/mol, respectively, indicate the existence of primarily physical effects, fairly weak chemical reactions, or a mix of physical and chemical effects, and strong chemical processes.[7,58] The E factor corresponding to the Cd(II) retention reactions by BEN, EXBEN, and Mth/EXBEN computed is consistent with the theoretical energies that are hypothesized for physical processes (8 to 16 kJ/mol) (Table 3).

2.4.4. Advanced Isotherm Modeling. Most recent advances in equilibrium mathematical models, which rely on the fundamentals of statistical physics hypotheses, possess the potential to offer substantial new insights into the distinctive attributes of adsorption operations, especially with regard to

https://doi.org/10.1021/acsomega.3c08592
ACS Omega 2024, 9, 11534−11550

the adsorbent-Cd(II) solution interfaces and the exterior features of these solid adsorbents. The statistical parameters obtained from these models, including steric and energy factors, may be used to clarify the mechanisms. Three primary parameters comprised the steric elements: the entire number of Cd(II) ions existing at each site ($n_{(Cd(II))}$); the total quantity of sites occupied by Cd(II) along the outside of BEN, EXBEN, and Mth/EXBEN ($N_{m(Cd(II))}$); and the maximum capacity of BEN, EXBEN, and Mth/EXBEN for capturing Cd(II) following full saturation ($Q_{sat(Cd(II))}$). Internal energy (E_{int}), free enthalpy (G), entropy (S_a), and Cd(II) eliminating energy (E) were the factors that were evaluated during the assessment of the energetic characteristics. The Cd(II) retention behaviors were analyzed by using a statistical model that was established. The model's illustrative equations were fitted nonlinearly to evaluate the degree of agreement with the model. Multivariable nonlinear regression computation was used in combination with the Levenberg−Marquardt iterative process to complete the fitting process. A monolayer model with a single energetic site was successfully used to investigate and characterize the adsorption processes of Cd(II) by BEN, EXBEN, and Mth/EXBEN on the basis of the provided levels of fitness (Table.3 and Figure 7A−C).

2.5. Steric Properties. *2.5.1. Number of Adsorbed MP ($n_{(Cd(II))}$) per Each Site.* The numerical results for the $n_{(Cd(II))}$ factor significantly indicate the orientation (horizontal or vertical) of the cadmium ions that have been retained on the BEN, EXBEN, and Mth/EXBEN interfaces. These findings have further consequences regarding the determination of the underlying mechanistic processes, specifically the differentiation between multidocking and multi-ionic. One Cd(II) ion is maintained by several sites of adsorption throughout horizontal arrangements in systems that are subject to multiple anchoring or multiple docking operations. A number of Cd(II) ions might be captured via a single site of binding across nonparallel and vertical orientations during activities with values greater than one; multi-ionic mechanistic operations are the primary cause of these retention characteristics.[7,59] The derived values of $n_{(Cd(II))}$ for BEN ($n_{(Cd(II))}$ = 1.33−1.4), EXBEN ($n_{(Cd(II))}$ = 1.8−2.2), and Mth/EXBEN ($n_{(Cd(II))}$ = 1.9−2.4) are more than 1 (Table 4 and Figure 7D−F). As a result, the Cd(II) ions were captured through multi-ionic processes. Each adsorbent retention site could hold up to two ions by BEN and three ions by EXBEN and Mth/EXBEN, which were then distributed vertically in a nonparallel manner. The reactivity of each site rose from 2 ions by BEN to 3 by EXBEN and Mth/EXBEN, confirming the noteworthy impact of the morphological modifications and methanol treatment on the binding affinity and reactivity of the existing active sites. The dramatically elevated reactivity of Mth/EXBEN may be due to their improved dispersion characteristics, contact interface, and surface reactivity that contribute to metal ion aggregation during their uptake by dominant active chemical groups. In terms of temperature effects, the computed $n_{(Cd(II))}$ values for BEN, EXBEN, and Mth/EXBEN display remarkable declination. This declared a significant diminishment in the aggregation behavior of Cd(II) ions during their adsorption.[2,60]

2.5.2. Occupied Active Sites Density (N_m). The density of cadmium-filled sites ($N_{m(Cd(II))}$) of BE, EXBEN, and Mth/EXBEN may be used to estimate the total number of binding sites that are accessible across the surfaces of these particulates during the course of the process. As shown in Figure 8G, the

Table 4. Mathematical Parameters of the Studied Advanced Isotherm Model

advanced isotherm model				
steric and energetic parameters				
		293 K	303 K	313 K
BEN	R^2	0.987	0.989	0.984
	χ^2	0.47	0.4	0.57
	n	1.4	1.36	1.33
	N_m (mg/g)	115.17	130.6	140.9
	Q_{sat} (mg/g)	161.23	177.6	187.39
	$C_{1/2}$ (mg/L)	53.1	47.9	41.7
	ΔE (kJ/mol)	9.03	8.78	8.44
EXBEN	R^2	0.997	0.999	0.988
	χ^2	0.17	0.06	0.78
	n	2.22	2.06	1.8
	N_m (mg/g)	115.4	132.6	162.9
	Q_{sat} (mg/g)	256.2	272.7	293.22
	$C_{1/2}$ (mg/L)	24.33	22.08	18.5
	ΔE (kJ/mol)	7.13	6.89	6.46
Mth/EXBEN	R^2	0.995	0.992	0.997
	χ^2	0.47	0.72	0.25
	n	2.42	2.1	1.97
	N_m (mg/g)	150.3	156.9	157.1
	Q_{sat} (mg/g)	363.7	329.4	309.4
	$C_{1/2}$ (mg/L)	20.2	24.3	28.2
	ΔE (kJ/mol)	−6.68	−7.13	−7.49

$N_{m(Cd(II))}$ levels determined for BEN are 115.7 at 293 K, 130.6 at 303 K, and 140.9 at 313 K (Figure 7G and Table 3). After exfoliation alterations (EXBEN) were applied, the results showed a slight improvement, reaching values of 115.4 mg/g (293 K), 132.6 mg/g (303 K), and 162.9 mg/g (313 K) (Figure 7H and Table 4). Furthermore, the availability of the active sites rose dramatically to 150.3 mg/g (293 K), 156.9 mg/g (303 K), and 157.1 mg/g (313 K) after the methanol modification of the exfoliating bentonite layers (Mth/EXBEN) (Figure 7I and Table 4). The findings confirm a significant increase in the total number of reactive sites after the exfoliating modification from 140.9 to 162.9 mg/g at the best temperature alongside the effect of the alcohol functioning stage which induces the active site density to 157 mg/g. Increased surface area, extended exposure of the chemically reactive siloxane groups, and the entrapment of various hydroxyl functional groups during the methanol implementation step, along with the silicate surface's increased reactivity due to its conversion into semicrystalline or amorphous materials, are the main factors causing this enhancement effect on the dominant adsorption sites. These modifications promote the establishment of an interactive contact across the exterior surfaces of Mth/EXBEN and EXBEN and the Cd(II) bearing solutions. Concerning the effect of temperature, the behaviors that were observed and the established filled active site density (N_m) by the retained cadmium ions show a general increase with increasing evaluating temperature utilizing BE, EXBEN, and Mth/EXBEN (Figure 7G−I). Regarding the temperature influence, this behavior is in excellent accord with the previously established patterns for the n parameter. The total number of filled adsorption sites significantly decreased as a consequence of the rise in aggregation activities throughout the adsorption of Cd(II) over the exteriors of BEN, EXBEN, and Mth/EXBEN.[2,61] Moreover, the high temperature conditions induce the ion

https://doi.org/10.1021/acsomega.3c08592
ACS Omega 2024, 9, 11534−11550

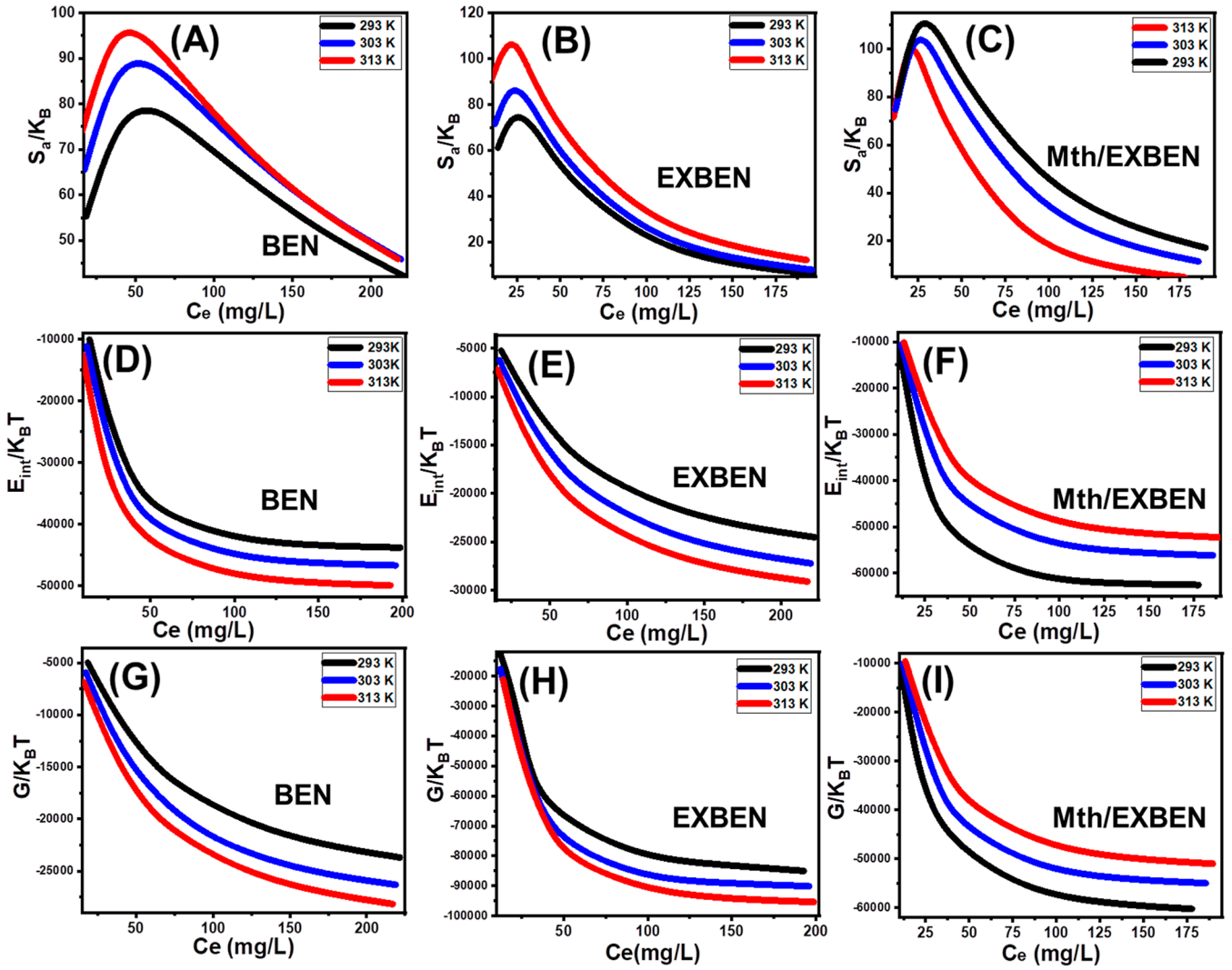

Figure 8. Change in entropy properties of Cd(II) adsorption with temperature [(A) BEN, (B) EXBEN, and (C) Mth/EXBEN]; change in the internal energy properties of Cd(II) adsorption with temperature [(D) BEN, (E) EXBEN, and (F) Mth/EXBEN]; and change in enthalpy properties of Cd(II) adsorption with temperature [(G) BEN, (H) EXBEN, and (I) Mth/EXBEN].

exchange properties within the bentonite structure or the free ions within the interlayer water molecules, which provide extra active sites during the uptake processes.[3]

2.5.3. Adsorption Capacity at the Saturation State of (Q_{sat}). The evaluation of Cd(II) retention characteristics of BEN, EXBEN, and Mth/EXBEN during the saturated state (Q_{sat}) provides the potential to attain the most precise estimation of their maximal adsorption capacities. The results of Q_{sat} are notably impacted by the determined densities of the occupied sites ($N_{m(Cd(II))}$) and the overall number of Cd(II) ions that filled each site ($n_{(Cd(II))}$). Bentonite, as a potential adsorbent for Cd(II), showed Q_{sat} values of 161.2 mg/g at 293 K, 177.6 mg/g at 303 K, and 187.4 mg/g at 313 K (Figure 7J and Table 3). The exfoliate product (EXBEN) has better retention characteristics across various temperature conditions. At a temperature of 293 K, the adsorption capacity reached a maximum value of 256.2 mg/g. The adsorption capacity at a temperature of 303 K has been measured as 272.7 mg/g, whereas at a temperature of 313 K, it has been determined to be 293.2 mg/g (Figure 7K and Table 4). The observed improvement significantly rose after the modification of the separated layers with methanol molecules (Mth/EXBEN), leading to quantities of 363.7 mg/g (293 K), 329.4 mg/g (303 K), and 309.4 mg/g (313 K) (Figure 7L and Table 4). The adverse effects of temperature ultimately indicate that Mth/EXBEN demonstrates exothermic behavior during the Cd(II) adsorption. This demonstrated how an elevated temperature accelerates the thermal collision features of the metal retention, lowering the efficacy of Cd(II) binding.[59] The uptake behavior of BEN and EXBEN displays a reverse effect as its saturation capacity of Cd(II) enhances notably with raising the level of the testing temperature; i.e., exhibits endothermic behavior. Moreover, the observed capabilities of Q_{sat} of BEN and EXBEN in relation to changes in retention temperature demonstrate a noteworthy agreement with the outlined characteristics of $N_{m(Cd(II))}$ when compared to $n_{(Cd(II))}$. This implies that the efficacy of Cd(II) retention is mostly influenced by the abundance of active sites rather than the potential capacity of each of the existing active sites throughout BEN and EXBEN. The reverse can be detected for the Q_{sat} of Cd(II) by Mth/EXBEN following the trend with temperature that appears to be dependent essentially on the reactivity and docking capacity of each active site rather than the overall quantities.

https://doi.org/10.1021/acsomega.3c08592
ACS Omega 2024, 9, 11534−11550

2.6. Energetic Properties. *2.6.1. Adsorption Energy.* The inspection of the energy variations (ΔE) corresponding to the elimination processes of Cd(II) might provide significant knowledge on the fundamental mechanisms involved, irrespective of whether they are influenced by physical or chemical aspects. Chemical pathways often have levels of energy beyond 80 kJ/mol, while physical processes normally maintain energies lower than 40 kJ/mol. Depending on the levels of retention energies, mechanistic activities that take place throughout physical processes can generally be categorized into a number of categories. The mechanisms being examined include hydrogen bonds, the effect of van der Waals forces, dipole−dipole reactions, coordination exchange, and hydrophobic bonds. These mechanisms have varying energy ranges, with hydrogen binding having a range of fewer than 30 kJ/mol, coordination exchange having a maximum energy of 40 kJ/mol, van der Waals spanning 4 to 10 kJ/mol, dipole−dipole having energies varying from 2 to 29 kJ/mol, and hydrophobic bonds having an energy of 5 kJ/mol.[55,62] The calculation and measurement of the uptake energy levels (ΔE) for Cd(II) have been successfully accomplished through utilization of eq 1. This equation necessitates various factors, including the established solubility of Cd(II) within the water-based solution being tested (S), the gas constant (R = 0.008314 kJ/mol K), the soluble Cd(II) concentrations across the half saturation states of BE, EXBEN, and Mth/EXBEN, as well as the actual temperature (T).[61]

$$\Delta E = RT \ln\left(\frac{S}{C}\right) \tag{1}$$

The established energies associated with the sequestration of Cd(II) using BEN and EXBEN lie within the ranges 8.4 to 9.3 and 6.4 to 7.13 kJ/mol, respectively. Conversely, the estimated values for Mth/BE extend from −6.6 to −8.49 kJ/mol. Therefore, the sequestration of Cd(II) using BEN, EXBEN, and Mth/EXBEN mostly occurred via physical processes that include dipole−dipole interactions (ranging from 2 to 29 kJ/mol), van der Waals forces (ranging from 4 to 10 kJ/mol), and hydrogen bonds (less than 30 kJ/mol). Furthermore, the positive values of ΔE seen in the Cd(II) capture processes by BEN and EXBEN align with the results obtained from the experiments performed on the endothermic characteristics of these processes. However, the negatively signed values for the obtained energies using Mth/EXBEN demonstrate the elimination of Cd(II) by exothermic processes.

2.7. Thermodynamic Functions. *2.7.1. Entropy.* The entropy (S_a) pertaining to the removal of Cd(II) using BEN, EXBEN, and Mth/EXBEN offers valuable insights into the order and disorder characteristics that characterize their particle surfaces under different Cd(II) concentrations and temperature settings. The S_a features have been highlighted using the earlier computed N_m and n values in conjunction with the Cd(II) levels at BEN, EXBEN, and Mth/EXBEN ($C_{1/2}$) half-saturation conditions according to eq 2.

$$\frac{S_a}{K_B} = N_m\left\{\ln\left(1 + \left(\frac{C}{C_{1/2}}\right)^n\right) - n\left(\frac{C}{C_{1/2}}\right)^n \frac{\ln\left(\frac{C}{C_{1/2}}\right)}{1 + \left(\frac{C}{C_{1/2}}\right)^n}\right\} \tag{2}$$

The obtained findings demonstrate a notable decrease in the entropy magnitudes (S_a) upon the uptake of Cd(II) with BEN, EXBEN, and Mth/EXBEN, especially at elevated levels of Cd(II). As the concentrations of Cd(II) ions rise, the trends show a considerable reduction in the disorder properties that characterize the BEN, EXBEN, and Mth/EXBEN interfaces (Figure 8A−C). The entropy observations also support the effective docking and binding of Cd(II) ions into the functioning active sites of BEN, EXBEN, and Mth/EXBEN, as well as the empty binding receptors, at low concentrations of cadmium ions.[61,63] During the investigation of the retention of Cd(II) by BEN, it was observed that the highest degrees of entropy could be obtained at equilibrium concentrations of 58.6 mg/L (293 K), 56.2 mg/L (303 K), and 53.7 mg/L (313 K). The equilibrium values of maximum entropy for EXBEN have been established to be 23.88 mg/g at 293 K, 22.6 mg/g at 303 K, and 20.9 mg/g at 313 K. The maximum entropy degrees observed throughout the use of Mth/EXBEN as an adsorbing material for Cd(II) ions are 19.6 mg/L (at a temperature of 293 K), 22.2 mg/L (at a temperature of 303 K), and 23.9 mg/L (at a temperature of 313 K). The equilibrium values exhibit a strong correlation with the predicted concentrations of Cd(II) under the conditions that are required for half-saturations of BEN, EXBEN, and Mth/EXBEN. As a result, the binding positions of Cd(II) ions became inaccessible for subsequent docking. Furthermore, the empirical findings prove a significant decrease in entropy values, suggesting a considerable decline in the number of vacant sites as well as a noticeable decrease in the attributes of freedom and migration provided by the Cd(II) ions.[64]

2.7.2. Internal Energy and Free Enthalpy. The present investigation intends to analyze the internal energy (E_{int}) corresponding to the retention of Cd(II) ions using three different materials: BE, EXBEN, and Mth/EXBEN. Furthermore, this research investigates the impact of fluctuations in the levels of Cd(II) on the free enthalpy (G) as well as the influence of temperature during testing. The evaluation is performed employing the parameters specified in eqs 3 and 4, which rely on the pre-established values of N_m, n, and $C_{1/2}$, together with the translation partition (Z_v).[60]

$$\frac{E_{int}}{K_B T} = nN_m\left[\left(\frac{\left(\frac{C}{C_{1/2}}\right)^n \ln\left(\frac{C}{Z_v}\right)}{1 + \left(\frac{C}{C_{1/2}}\right)^n}\right) - \left(\frac{n \ln\left(\frac{C}{C_{1/2}}\right)\left(\frac{C}{C_{1/2}}\right)^n}{1 + \left(\frac{C}{C_{1/2}}\right)^n}\right)\right] \tag{3}$$

$$\frac{G}{K_B T} = nN_m \frac{\ln\left(\frac{C}{Z_v}\right)}{1 + \left(\frac{C_{1/2}}{C}\right)^n} \tag{4}$$

The computed internal energy (E_{int}) results for the removal processes of Cd(II) by BE, EXBEN, and Mth/EXBEN demonstrate negatively signed values (Figure 8D−F). The findings of the present investigation demonstrate a significant decrease in internal energy (E_{int}) when the operational temperature is increased from 293 to 313 K for Mth/EXBEN while the reverse occurs for BE and EXBEN. As a result, the adsorption procedures of Mth/EXBEN for Cd(II) exhibit spontaneous and exothermic behaviors within the assessed experimental ranges while the uptake by BE and EXBEN displays spontaneous and endothermic behaviors. Comparable behaviors and characteristics have been found for the predetermined enthalpy values. The G values demonstrate a downward trend and show reversible correlations with the

https://doi.org/10.1021/acsomega.3c08592
ACS Omega 2024, 9, 11534−11550

tracked temperature for Mth/EXBEN and enhance with temperature for BE and EXBEN (Figure 8G–I). This suggests a decline in the feasibility features with temperature for the Mth/EXBEN adsorption system for Cd(II) and enhancement in the feasibility and freedom properties of the BE and EXBEN adsorption systems. The aforementioned finding provides support for the inherent spontaneity and exothermicity of the uptake of Cd(II) by Mth/EXBEN and the endothermicity for BE and EXBEN.

2.8. Recyclability. The key objective of conducting the reusability experiments was to evaluate the appropriateness of the developed EXBEN and Mth/EXBEN for application in economic- and industrial-scale activities. The EXBEN and Mth/EXBEN particles were regenerated using a washing technique including immersion in a diluted NH_4Cl solution (1 moL) for a period of 10 min. The elution process as well as the desorption of the capturing Cd(II) ions was facilitated by using a magnetic stirrer. Following this, the tiny particles were separated via the process of filtration and then underwent an additional washing procedure using distilled water for a period of 10 min. Subsequently, the particles were subjected to a drying process lasting 12 h at a temperature of 65 °C in preparation for their further use in the reuse of adsorption cycles. The reuse experiments were carried out for five repetitions, considering the removal effectiveness of Cd(II) ions. The experimental variables that were manipulated were the solid dosage (0.2 g/L), duration (24 h), volume (100 mL), concentration (100 mg/L), and temperature (293 K). According to the experimental results on the elimination performance of Cd(II) ions, Mth/EXBEN and EXBEN show high stability and significant potential for recycling as adsorbents. Regarding the reusing of EXBEN during the capture of Cd(II) ions, it was observed that the material had an elimination capacity of more than 250.2 mg/g during two cycles, surpassing 240 mg/g during three cycles, and beyond 225 mg/g during the course of five cycles (Figure 9). During

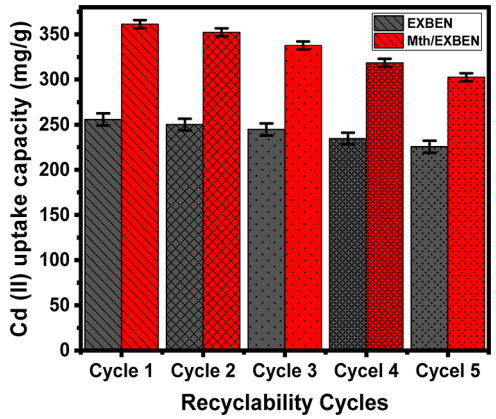

Figure 9. Recyclability properties of EXBEN and Mth/EXBEN as adsorbents for Cd(II) ions.

the process of eliminating Cd(II) ions, the recyclable potential of Mth/EXBEN has been observed. The documented elimination capabilities have been shown to exceed 352.4 over the course of two cycles, beyond 335 mg/g over three cycles, and above 300 mg/g over five cycles (Figure 9). The decrease in the efficiency of Cd(II) ion removal using EXBEN and Mth/EXBEN materials, seen via a linear fall, may be explained by the continuous formation of complexes between adsorbed Cd(II) ions and reactive groups that are found throughout the structure of EXBEN and Mth/EXBEN. This effect becomes more pronounced with a rise in the number of recyclable and reuse rounds. The establishment of these complexes results in a reduction in the quantity of available vacant sites during adsorption.

2.9. Comparison Study. The existing capabilities of BEN and EXBEN were assessed compared with the Cd(II) adsorption qualities of other examined adsorbents in the literature. The measured effectiveness of BEN and EXBEN exceeded the stated values of several adsorbents that have been examined before such as clay (vermiculite, attapulgite, bentonite), CNTs (maghemite/MWCNTs, oxidized CNTs, and MnO_2/MWCNTs), activated carbon, graphene oxide, biochar, mesoporous silica (MCM-41/thioglycolic acid, SBA-15, MCM-48, Ti-MCM-48), zeolite (β-cyclodextrin/zeolite and zeolite/zerovalent iron), hydroxyapatite, and chitosan adsorbents (Table.5).

Table 5. Comparison Study for the Adsorption Capacities of the Synthetic Structure and Other Studies' Adsorbents

adsorbent	Q_{max} (mg/g)	refs
maghemite/MWCNTs	78.18	65
magnetic MCM-48	114.08	66
MCM-41/thioglycolic acid	91.3	67
amino functional SBA-15	93.3	68
Fe_3O_4-chitosan@bentonite	62.1	69
zeolite/zerovalent iron (Z-NZVI)	62.02	70
graphene oxide	23.9	71
MnO_2/MWCNTs	41.6	72
oxidized CNTs	92.59	73
Ti-MCM-48	83.57	74
Canna indica based biochar	140.01	75
composite chitosan biosorbent	108.7	76
β-cyclodextrin/zeolite	93.06	77
MCM-48	79.3	78
attapulgite/$CoFe_2O_4$@SiO_2-chitosan/EDTA	127.79	79
activated carbon	26.36	80
chitosan/vermiculite	58.48	81
magnetic chitosan-phenylthiourea resin	120	82
BEN	363.7	this study
EXBEN	293.2	this study

3. CONCLUSIONS

The natural bentonite (BE) was effectively scrubbed into individual silicate sheets (EXBE) and subsequently modified with methanol, resulting in methoxy exfoliating bentonite (Mth/EXBEN). These modified materials demonstrate improved adsorption properties for Cd(II) metallic ions. The Cd(II) retention qualities have been studied in a synergetic, comprehensive investigation implementing both steric and energetic characteristics. The Mth/EXBEN structure demonstrates a greater capacity (363.7 mg/g) compared with EXBEN (293.2 mg/g) and BEN (187.3 mg/g), indicating that the exfoliating and methanol-functioning operations have beneficial effects on the physicochemical and surficial aspects of bentonite. The modification activities led to an increase in surface area, as well as the integration of extra empty and active sites. This finding was corroborated by the computed density of active sites (N_m). The respective values of N_m were determined to be 157.1 (Mth/EXBEN), 162.9 (EXBEN), and

https://doi.org/10.1021/acsomega.3c08592
ACS Omega 2024, 9, 11534−11550

140.9 mg/g (BEN). The obtained energetic results, encompassing Gaussian energy (less than 8 kJ/mol) as well as retention energy (less than 40 kJ/mol), indicate that there were no substantial alterations detected in the physical adsorption pathways (specifically, dipole forces along with hydrogen binding) after the different modification steps. The evaluated mechanism occurred spontaneously with exothermic characteristics using Mth/EXBEN and endothermic characteristics using BEN and EXBEN.

4. EXPERIMENTAL WORK

4.1. Materials. The specimens of the bentonite precursor were collected from a naturally occurring bentonite quarry located in the Western Desert of Egypt. The composition of the samples is as follows: 54.82% SiO_2, 2.5% MgO, 9.5% Fe_2O_3, 17.56% Al_2O_3, 2.4% CaO, 2.6% Na_2O, 1.45% TiO_2, and 9.2% LOI. The ingredients utilized in the various production protocols include sodium fluoride (NaF), sodium hexametaphosphate ($(NaPO_3)_6$), dimethyl sulfoxide (DMSO), and methanol. All of the chemicals utilized in the exfoliating operations and methanol modification phases were of laboratory standards and had been obtained from Sigma-Aldrich, Egypt. The adsorption experiments employed a standard solution of Cd(II) with a proven concentration of 1000 mg/L that was procured from the Sigma-Aldrich Company in Egypt.

4.2. Synthesis of Methoxy Exfoliated Bentonite. The typical exfoliation approaches for bentonite were carried out using the liquid-phase stripping method. Initially, a quantity of 10 g of finely powdered bentonite was thoroughly mixed with a solution of sodium fluoride (0.4 g) in 200 mL of water. This mixture was subjected to continuous stirring at a rate of 500 rpm for a duration of 90 min while maintaining the external temperature at approximately 80 °C. The slurry that had resulted earlier was further reinforced with $(NaPO_3)_6$ (0.05 g) and thereafter subjected to ultrasonic irradiation for a duration of 120 min at a power level of 240 W. After the sonication process, the resulting supernatant was allowed to settle at ambient temperature for a duration of 24 h prior to undergoing centrifugation at a high speed for a period of 30 min (at 5000 rpm). This centrifugation step aimed to isolate the bentonite-like colloidal flakes, which represent the exfoliating material (EXBEN). Subsequently, the rinsed EXBEN was mixed with 100 mL of methanol for 48 h inside a glass autoclave at ambient temperature. The process of blending EXBEN with methanol was accomplished using a magnetic stirring apparatus operating at a speed of 500 rpm and an ultrasonic source with a power output of 240 W. Consequently, the product was extracted from the residual solutions and afterward underwent an extensive washing procedure. Subsequently, the sample was subjected to a delicate drying process at a temperature of 50 °C for 12 h. Following this, it was appropriately labeled as Mth/MXBEN in order to facilitate its integration into further stages of characterization and investigation.

4.3. Analytical Techniques. The levels of crystallization and phase recognition of crystals have been evaluated using a PANalytical-Empyrean X-ray diffractometer. This instrument has a measurement range spanning from 0 to 70° and was utilized to analyze the XRD patterns obtained. The nature of the chemical groups found in EXBEN and Mth/EXBEN was determined by the utilization of a Fourier transform infrared spectrometer (FTIR8400S; Shimadzu) that has a detectable wavelength spectrum spanning from 400 to 4000 cm^{-1}. This analysis allowed for a comparison of these functional groups with those present in raw bentonite prior to the modifications. Through the study of SEM photos, the morphological characteristics of EXBEN and Mth/EXBEN were investigated in comparison with those of starting bentonite. The images were acquired using the scanning electron microscope (Gemini, Zeiss-Ultra 55) subsequent to the implantation of very thin films of gold onto the outside surfaces of EXBEN and Mth/EXBEN. Furthermore, an evaluation has been carried out on the intrinsic properties through the examination of their HRTEM photographs. The images were obtained with a JEOL-JEM2100 transmission electron microscope that was operated at an accelerating voltage of 200 kV. A surface area analyzer (Beckman Coulter SA3100) was employed to measure the porosity and surface area of EXBEN and Mth/EXBEN. This was achieved by examining the N_2 adsorption as well as desorption isotherms specific to each material at −196 °C after degassing step at 90 °C for 12 h.

4.4. Adsorption Studies. Adsorption procedures for eliminating cadmium ions (Cd(II)) employing BE, EXBEN, and Mth/EXBEN were implemented in the batch testing. The research used established experimental variables, such as pH levels spanning from 2 to 7, retention durations ranging from 20 to 300 min, and varying concentrations of Cd(II) ranging from 25 to 250 mg/L. Furthermore, the experimental conditions included the manipulation of the evaluating temperature, which was systematically altered between the values of 293 and 313 K. In addition, the remaining key testing factors were meticulously chosen and consistently upheld at predetermined values throughout the duration of the study [volume: 100 mL; solid dosage: 0.2 g/L]. The setups of the experiment have been analyzed three times, utilizing the mean values of all determined concentrations in addition to any subsequent calculations or inspections. After the adsorption trials reached a state of equilibrium, the solid particulates of BE, EXBEN, and Mth/EXBEN were separated from the Cd(II) solutions using Whatman filter papers. The level of Cd(II) left in the treated solutions was determined using inductively coupled plasma mass spectrometry (ICP-MS) equipment supplied by PerkinElmer. The Cd(II) standard utilized in the analysis has been validated by the National Standard & Technology Institute (NIST), whereas the reference standard was purchased through Merck Company (Germany). The calculation of the adsorption capacities (Q_e) of Cd(II) ions via BE, EXBEN, and Mth/EXBEN was accomplished in mg/g employing eq 5. The computation considered many factors, including the solutions, volume (V) in milliliters, and dosages of BE, EXBEN, and Mth/EXBEN (m) in mg, the initial level of Cd(II) (C_o) in mg/L, and the residual content of Cd(II) (C_e) in mg/L.

$$Q_e\ (\mathrm{mg/g}) = \frac{(C_o - C_e)V}{m} \tag{5}$$

4.5. Theoretical Traditional and Advanced Equilibrium Studies. The adsorption tests have been modeled using several approaches to modeling, including normal kinetic, standard isotherm, and more advanced equilibrium models. These models were developed based on assertions adapted from the theories of statistical physics (Table S1). Nonlinear regression methodologies were employed to simulate the kinetic and classical equilibrium models. The analysis adopted the mathematical formulas of the previously

https://doi.org/10.1021/acsomega.3c08592
ACS Omega 2024, 9, 11534−11550

described models. The main markers of the fitting levels were derived according to correlation coefficients (R^2) (eq 6) alongside Chi-squared (χ^2) (eq 7). The evaluation of the alignment between the uptake activities' matching levels and the evaluated advanced equilibrium models was conducted across the assessment of the coefficient of correlation (R^2) and the root-mean-square error (RMSE) (eq 8). The number of experimental results is denoted by the letter m', the number of studied parameters that were analyzed is denoted by p, the predicted sequestration of Cd(II) is denoted by Qi_{cal}, and the confirmed capacity for Cd(II) sequestration is denoted by Qi_{exp}.

$$R^2 = 1 - \frac{\sum (q_{e,exp} - q_{e,cal})^2}{\sum (q_{e,exp} - q_{e,mean})^2} \quad (6)$$

$$\chi^2 = \sum \frac{(q_{e,exp} - q_{e,cal})^2}{q_{e,cal}} \quad (7)$$

$$RMSE = \sqrt{\frac{\sum_{i=1}^{m} (Qi_{cal} - Qi_{exp})^2}{m' - p}} \quad (8)$$

■ ASSOCIATED CONTENT

Supporting Information

The Supporting Information is available free of charge at https://pubs.acs.org/doi/10.1021/acsomega.3c08592.

The Supporting Information includes the representative equations of the kinetic and isotherm models (PDF)

■ AUTHOR INFORMATION

Corresponding Authors

Mostafa R. Abukhadra − *Geology Department, Faculty of Science, Beni-Suef University, Beni Suef City 62511, Egypt; Materials Technologies and Their Applications Lab, Faculty of Science, Beni-Suef University, Beni Suef City 62511, Egypt;* orcid.org/0000-0001-5404-7996; Phone: +2001288447189; Email: Abukhadra89@Science.bsu.edu.eg

Wail Al Zoubi − *Materials Electrochemistry Laboratory, School of Materials Science and Engineering, Yeungnam University, Gyeongsan 38541, Republic of Korea;* orcid.org/0000-0003-4213-8481; Email: wailalzoubi@ynu.ac.kr

Authors

Nourhan Nasser − *Geology Department, Faculty of Science, Beni-Suef University, Beni Suef City 62511, Egypt; Materials Technologies and Their Applications Lab, Faculty of Science, Beni-Suef University, Beni Suef City 62511, Egypt*

Ahmed M. El-Sherbeeny − *Industrial Engineering Department, College of Engineering, King Saud University, Riyadh 11421, Saudi Arabia;* orcid.org/0000-0003-3559-6249

Complete contact information is available at: https://pubs.acs.org/10.1021/acsomega.3c08592

Author Contributions

This article was written through the contributions of all authors. All authors have given approval to the final version of the manuscript.

Notes

The authors declare no competing financial interest.

Recommendation: Further studies will be conducted to follow the physicochemical and technical properties of the spent adsorbents after the retention cycles to qualify them for different industrial and environmental applications.

■ ACKNOWLEDGMENTS

The authors extend their appreciation to King Saud University for funding this work through Researchers Supporting Project number (RSP2024R133), King Saud University, Riyadh, Saudi Arabia.

■ REFERENCES

(1) Sajid, M.; Sajid Jillani, S. M.; Baig, N.; Alhooshani, K. Layered Double Hydroxide-Modified Membranes for Water Treatment: Recent Advances and Prospects. *Chemosphere* **2022**, *287*, 132140.

(2) Yang, X.; Wang, J.; El-Sherbeeny, A. M.; AlHammadi, A. A.; Park, W.-H.; Abukhadra, M. R. Insight into the Adsorption and Oxidation Activity of a ZnO/Piezoelectric Quartz Core-Shell for Enhanced Decontamination of Ibuprofen: Steric, Energetic, and Oxidation Studies. *Chem. Eng. J.* **2022**, *431*, 134312.

(3) Abdel Salam, M.; Mokhtar, M.; Albukhari, S. M.; Baamer, D. F.; Palmisano, L.; Jaremko, M.; Abukhadra, M. R. Synthesis and Characterization of Green ZnO@polynaniline/Bentonite Tripartite Structure (G.Zn@PN/BE) as Adsorbent for As (V) Ions: Integration, Steric, and Energetic Properties. *Polymers* **2022**, *14* (12), 2329.

(4) Velarde, L.; Nabavi, M. S.; Escalera, E.; Antti, M.-L.; Akhtar, F. Adsorption of Heavy Metals on Natural Zeolites: A Review. *Chemosphere* **2023**, *328*, 138508.

(5) Mashkoor, F.; Shoeb, M.; Mashkoor, R.; Anwer, A. H.; Zhu, S.; Jeong, H.; Baek, S.-S.; Jung, J.; Jeong, C. Synergistic Effects of Tungstate Trioxide Hemihydrate Decorated Reduced Graphene Oxide for the Adsorption of Heavy Metals and Dyes and Postliminary Application in Supercapacitor Device. *J. Cleaner Prod.* **2023**, *418*, 138067.

(6) Javaheri, F.; Kheshti, Z.; Ghasemi, S.; Altaee, A. Enhancement of Cd2+ Removal from Aqueous Solution by Multifunctional Mesoporous Silica: Equilibrium Isotherms and Kinetics Study. *Sep. Purif. Technol.* **2019**, *224*, 199−208.

(7) Sayed, I. R.; Farhan, A. M.; AlHammadi, A. A.; El-Sayed, M. I.; Abd El-Gaied, I. M.; El-Sherbeeny, A. M.; Al Zoubi, W.; Ko, Y. G.; Abukhadra, M. R. Synthesis of Novel Nanoporous Zinc Phosphate/Hydroxyapatite Nano-Rods (ZPh/HPANRs) Core/Shell for Enhanced Adsorption of Ni2+ and Co2+ Ions: Characterization and Application. *J. Mol. Liq.* **2022**, *360*, 119527.

(8) Igiri, B. E.; Okoduwa, S. I. R.; Idoko, G. O.; Akabuogu, E. P.; Adeyi, A. O.; Ejiogu, I. K. Toxicity and Bioremediation of Heavy Metals Contaminated Ecosystem from Tannery Wastewater: A Review. *J. Toxicol.* **2018**, *2018*, 1−16.

(9) Nasser, N.; El-Sayed, M. I.; Othman, S. I.; Allam, A. A.; Al-Labadi, I. G.; Abukhadra, M. R.; Bellucci, S. Systematic Evaluation for the Impact of the Geological Conditions on the Adsorption Affinities of Calcite as an Adsorbent of Zn2+ Ions from Aqueous Solutions: Experimental and Theoretical Studies. *Minerals* **2022**, *12* (12), 1635.

(10) O'Connor, K. F.; Al-Abed, S. R.; Horden, S.; Pinto, P. X. Assessing the Efficiency and Mechanism of Zinc Adsorption Onto Biochars from Poultry Litter and Softwood Feedstocks. *Bioresour. Technol. Rep.* **2022**, *18*, 101039.

(11) Brandes, R.; Belosinschi, D.; Brouillette, F.; Chabot, B. A New Electrospun Chitosan/Phosphorylated Nanocellulose Biosorbent for the Removal of Cadmium Ions from Aqueous Solutions. *J. Environ. Chem. Eng.* **2019**, *7* (6), 103477.

(12) Shaban, M.; Abukhadra, M. R. Geochemical Evaluation and Environmental Application of Yemeni Natural Zeolite as Sorbent for Cd2+ from Solution: Kinetic Modeling, Equilibrium Studies, and Statistical Optimization. *Environ. Earth Sci.* **2017**, *76* (8), 310.
(13) Vilela, P. B.; Matias, C. A.; Dalalibera, A.; Becegato, V. A.; Paulino, A. T. Polyacrylic Acid-Based and Chitosan-Based Hydrogels for Adsorption of Cadmium: Equilibrium Isotherm, Kinetic and Thermodynamic Studies. *J. Environ. Chem. Eng.* **2019**, *7* (5), 103327.
(14) Abolfazli Behrooz, B.; Oustan, S.; Mirseyed Hosseini, H.; Etesami, H.; Padoan, E.; Magnacca, G.; Marsan, F. A. The Importance of Presoaking to Improve the Efficiency of MgCl2-Modified and Non-Modified Biochar in the Adsorption of Cadmium. *Ecotoxicol. Environ. Saf.* **2023**, *257*, 114932.
(15) Souza-Arroyo, V.; Fabián, J. J.; Bucio-Ortiz, L.; Miranda-Labra, R. U.; Gomez-Quiroz, L. E.; Gutiérrez-Ruiz, M. C. The Mechanism of the Cadmium-Induced Toxicity and Cellular Response in the Liver. *Toxicology* **2022**, *480*, 153339.
(16) El Rasafi, T.; Oukarroum, A.; Haddioui, A.; Song, H.; Kwon, E. E.; Bolan, N.; Tack, F. M. G.; Sebastian, A.; Prasad, M. N. V.; Rinklebe, J. Cadmium Stress in Plants: A Critical Review of the Effects, Mechanisms, and Tolerance Strategies. *Crit. Rev. Environ. Sci. Technol.* **2022**, *52* (5), 675−726.
(17) Abukhadra, M. R.; Mostafa, M.; Jumah, M. N. B.; Al-Khalawi, N.; Alruhaimi, R. S.; Salama, Y. F.; Allam, A. A. Insight into the Adsorption Properties of Chitosan/Zeolite-A Hybrid Structure for Effective Decontamination of Toxic Cd (II) and As (V) Ions from the Aqueous Environments. *J. Polym. Environ.* **2022**, *30* (1), 295−307.
(18) Ofudje, E. A.; Adedapo, A. E.; Oladeji, O. B.; Sodiya, E. F.; Ibadin, F. H.; Zhang, D. Nano-Rod Hydroxyapatite for the Uptake of Nickel Ions: Effect of Sintering Behaviour on Adsorption Parameters. *J. Environ. Chem. Eng.* **2021**, *9* (5), 105931.
(19) El-Sherbeeny, A. M.; Ibrahim, S. M.; AlHammadi, A. A.; Soliman, A. T. A.; Shim, J.-J.; Abukhadra, M. R. Effective retention of radioactive Cs+ and Ba2+ ions using β-cyclodextrin functionalized diatomite (β-CD/D) as environmental adsorbent; characterization, application, and safety. *Surf. Interfaces* **2021**, *26*, 101434.
(20) Kadeche, A.; Ramdani, A.; Adjdir, M.; Guendouzi, A.; Taleb, S.; Kaid, M.; Deratani, A. Preparation, Characterization and Application of Fe-Pillared Bentonite to the Removal of Coomassie Blue Dye from Aqueous Solutions. *Res. Chem. Intermed.* **2020**, *46* (11), 4985−5008.
(21) Chen, Y.; Nie, Z.; Gao, J.; Wang, J.; Cai, M. A Novel Adsorbent of Bentonite Modified Chitosan-Microcrystalline Cellulose Aerogel Prepared by Bidirectional Regeneration Strategy for Pb(II) Removal. *J. Environ. Chem. Eng.* **2021**, *9* (4), 105755.
(22) Yu, H.; Li, C.; Yan, J.; Ma, Y.; Zhou, X.; Yu, W.; Kan, H.; Meng, Q.; Xie, R.; Dong, P. A Review on Adsorption Characteristics and Influencing Mechanism of Heavy Metals in Farmland Soil. *RSC Adv.* **2023**, *13* (6), 3505−3519.
(23) Raju, C. H. A. I.; Anitha, J.; Mahalakshmi Kalyani, R.; Satyanandam, K.; Jagadeesh, P. Sorption of Cobalt Using Marine Macro Seaweed Graciliariacorticatared Algae Powder. *Mater. Today: Proc.* **2021**, *44*, 1816−1827.
(24) Momina; Mohammad, S.; Suzylawati, I. Study of the Adsorption/Desorption of MB Dye Solution Using Bentonite Adsorbent Coating. *J. Water Proc. Eng.* **2020**, *34*, 101155.
(25) Abukhadra, M. R.; Saad, I.; Othman, S. I.; Allam, A. A.; Fathallah, W. Synthesis of Co3O4 @ Organo/Polymeric Bentonite Structures as Environmental Photocatalysts and Antibacterial Agents for Enhanced Removal of Methyl Parathion and Pathogenic Bacteria. *J. Inorg. Organomet. Polym. Mater.* **2022**, *32* (7), 2600−2614.
(26) Dardir, F. M.; Mohamed, A. S.; Abukhadra, M. R.; Ahmed, E. A.; Soliman, M. F. Cosmetic and Pharmaceutical Qualifications of Egyptian Bentonite and Its Suitability as Drug Carrier for Praziquantel Drug. *Eur. J. Pharm. Sci.* **2018**, *115*, 320−329.
(27) Liu, H.; Fu, T.; Sarwar, M. T.; Yang, H. Recent Progress in Radionuclides Adsorption by Bentonite-Based Materials as Ideal Adsorbents and Buffer/Backfill Materials. *Appl. Clay Sci.* **2023**, *232*, 106796.
(28) Ain, Q. U.; Rasheed, U.; Yaseen, M.; Zhang, H.; He, R.; Tong, Z. Fabrication of Magnetically Separable 3-Acrylamidopropyltrimethylammonium Chloride Intercalated Bentonite Composite for the Efficient Adsorption of Cationic and Anionic Dyes. *Appl. Surf. Sci.* **2020**, *514*, 145929.
(29) Almahri, A. The Solid-State Synthetic Performance of Bentonite Stacked Manganese Ferrite Nanoparticles: Adsorption and Photo-Fenton Degradation of MB Dye and Antibacterial Applications. *J. Mater. Res. Technol.* **2022**, *17*, 2935−2949.
(30) Meng, B.; Guo, Q.; Men, X.; Ren, S.; Jin, W.; Shen, B. Modified Bentonite by Polyhedral Oligomeric Silsesquioxane and Quaternary Ammonium Salt and Adsorption Characteristics for Dye. *J. Saudi Chem. Soc.* **2020**, *24* (3), 334−344.
(31) Gong, X.-L.; Lu, H.-Q.; Li, K.; Li, W. Effective Adsorption of Crystal Violet Dye on Sugarcane Bagasse-Bentonite/Sodium Alginate Composite Aerogel: Characterisation, Experiments, and Advanced Modelling. *Sep. Purif. Technol.* **2022**, *286*, 120478.
(32) Ashiq, A.; Walpita, J.; Vithanage, M. Functionalizing Non-Smectic Clay via Methoxy-Modification for Enhanced Removal and Recovery of Oxytetracycline from Aqueous Media. *Chemosphere* **2021**, *276*, 130079.
(33) Tan, D.; Yuan, P.; Dong, F.; He, H.; Sun, S.; Liu, Z. Selective Loading of 5-Fluorouracil in the Interlayer Space of Methoxy-Modified Kaolinite for Controlled Release. *Appl. Clay Sci.* **2018**, *159*, 102−106.
(34) Tchoumene, R.; Kenne Dedzo, G.; Ngameni, E. Intercalation of 1,2,4-Triazole in Methanol Modified-Kaolinite: Application for Copper Corrosion Inhibition in Concentrated Sodium Chloride Aqueous Solution. *J. Solid State Chem.* **2022**, *311*, 123103.
(35) Li, X.; Cui, X.; Wang, S.; Wang, D.; Li, K.; Liu, Q.; Komarneni, S. Methoxy-Grafted Kaolinite Preparation by Intercalation of Methanol: Mechanism of Its Structural Variability. *Appl. Clay Sci.* **2017**, *137*, 241−248.
(36) Borah, A.; Borah, A. R.; Gogoi, M.; Goswami, R.; Hazarika, S. Organic Exfoliation of Hydrophilic Bentonite Using Aliquat 336 and Isobutyl(Trimethoxy)Silane to Enhance Its Activity Toward pH-Dependent Adsorption of Epigallocatechin Gallate. *Clays Clay Miner.* **2023**, *71* (4), 430−447.
(37) Abukhadra, M. R.; Bakry, B. M.; Adlii, A.; Yakout, S. M.; El-Zaidy, M. E. Facile Conversion of Kaolinite into Clay Nanotubes (KNTs) of Enhanced Adsorption Properties for Toxic Heavy Metals (Zn2+, Cd2+, Pb2+, and Cr6+) from Water. *J. Hazard. Mater.* **2019**, *374*, 296−308.
(38) Abukhadra, M. R.; Mostafa, M.; El-Sherbeeny, A. M.; El-Meligy, M. A.; Nadeem, A. Instantaneous Adsorption of Synthetic Dyes from an Aqueous Environment Using Kaolinite Nanotubes: Equilibrium and Thermodynamic Studies. *ACS Omega* **2021**, *6* (1), 845−856.
(39) Alqahtani, M. D.; Nasser, N.; Bin Jumah, M. N.; AlZahrani, S. A.; Allam, A. A.; Abukhadra, M. R.; Bellucci, S. Insight into the Morphological Properties of Nano-Kaolinite (Nanoscrolls and Nanosheets) on Its Qualification as Delivery Structure of Oxaliplatin: Loading, Release, and Kinetic Studies. *Molecules* **2023**, *28* (13), 5158.
(40) Shawky, A.; El-Sheikh, S. M.; Rashed, M. N.; Abdo, S. M.; El-Dosoqy, T. I. Exfoliated Kaolinite Nanolayers as an Alternative Photocatalyst with Superb Activity. *J. Environ. Chem. Eng.* **2019**, *7* (3), 103174.
(41) Tian, L.; Abukhadra, M. R.; Mohamed, A. S.; Nadeem, A.; Ahmad, S. F.; Ibrahim, K. E. Insight into the Loading and Release Properties of an Exfoliated Kaolinite/Cellulose Fiber (EXK/CF) Composite as a Carrier for Oxaliplatin Drug: Cytotoxicity and Release Kinetics. *ACS Omega* **2020**, *5* (30), 19165−19173.
(42) Tang, R.; Xu, S.; Hu, Y.; Wang, J.; Lu, C.; Wang, L.; Zhou, Z.; Liao, D.; Zhang, H.; Tong, Z. Multifunctional Nano-Cellulose Aerogel for Efficient Oil-Water Separation: Vital Roles of Magnetic Exfoliated Bentonite and Polyethyleneimine. *Sep. Purif. Technol.* **2023**, *314*, 123557.
(43) Abukhadra, M. R.; Refay, N. M.; El-Sherbeeny, A. M.; Mostafa, A. M.; Elmeligy, M. A. Facile Synthesis of Bentonite/Biopolymer

https://doi.org/10.1021/acsomega.3c08592
ACS Omega 2024, 9, 11534−11550

Composites as Low-Cost Carriers for 5-Fluorouracil Drug; Equilibrium Studies and Pharmacokinetic Behavior. *Int. J. Biol. Macromol.* **2019**, *141*, 721−731.
(44) Abukhadra, M. R.; Allah, A. F. Synthesis and Characterization of Kaolinite Nanotubes (KNTs) as a Novel Carrier for 5-Fluorouracil of High Encapsulation Properties and Controlled Release. *Inorg. Chem. Commun.* **2019**, *103*, 30−36.
(45) Vivas, E. L.; Cho, K. Efficient Adsorptive Removal of Cobalt(II) Ions from Water by Dicalcium Phosphate Dihydrate. *J. Environ. Manage.* **2021**, *283*, 111990.
(46) Salam, M. A.; Abukhadra, M. R.; Mostafa, M. Effective Decontamination of As(V), Hg(II), and U(VI) Toxic Ions from Water Using Novel Muscovite/Zeolite Aluminosilicate Composite: Adsorption Behavior and Mechanism. *Environ. Sci. Pollut. Res.* **2020**, *27* (12), 13247−13260.
(47) Jiang, Y.; Abukhadra, M. R.; Refay, N. M.; Sharaf, M. F.; El-Meligy, M. A.; Awwad, E. M. Synthesis of chitosan/MCM-48 and β-cyclodextrin/MCM-48 composites as bio-adsorbents for environmental removal of Cd2+ ions; kinetic and equilibrium studies. *React. Funct. Polym.* **2020**, *154*, 104675.
(48) Abukhadra, M. R.; Saad, I.; Al Othman, S. I.; Alfassam, H. E.; Allam, A. A. Insight into the Synergetic, Steric and Energetic Properties of Zeolitization and Cellulose Fiber Functionalization of Diatomite during the Adsorption of Cd(Ii): Advanced Equilibrium Studies. *RSC Adv.* **2023**, *13* (34), 23601−23618.
(49) El Qada, E. Kinetic Behavior of the Adsorption of Malachite Green UsingJordanian Diatomite as Adsorbent. *Jordanian J. Eng. Chem. Ind.* **2020**, *3* (1), 1−10.
(50) Lin, X.; Xie, Y.; Lu, H.; Xin, Y.; Altaf, R.; Zhu, S.; Liu, D. Facile Preparation of Dual La-Zr Modified Magnetite Adsorbents for Efficient and Selective Phosphorus Recovery. *Chem. Eng. J.* **2021**, *413*, 127530.
(51) Albukhari, S. M.; Salam, M. A.; Abukhadra, M. R. Effective Retention of Inorganic Selenium Ions (Se (VI) and Se (IV)) Using Novel Sodalite Structures from Muscovite; Characterization and Mechanism. *J. Taiwan Inst. Chem. Eng.* **2021**, *120*, 116−126.
(52) Sherlala, A. I. A.; Raman, A. A. A.; Bello, M. M.; Buthiyappan, A. Adsorption of Arsenic Using Chitosan Magnetic Graphene Oxide Nanocomposite. *J. Environ. Manage.* **2019**, *246*, 547−556.
(53) Huang, Y.; Zeng, X.; Guo, L.; Lan, J.; Zhang, L.; Cao, D. Heavy Metal Ion Removal of Wastewater by Zeolite-Imidazolate Frameworks. *Sep. Purif. Technol.* **2018**, *194*, 462−469.
(54) Jasper, E. E.; Ajibola, V. O.; Onwuka, J. C. Nonlinear Regression Analysis of the Sorption of Crystal Violet and Methylene Blue from Aqueous Solutions onto an Agro-Waste Derived Activated Carbon. *Appl. Water Sci.* **2020**, *10* (6), 132.
(55) Ashraf, M.-T.; AlHammadi, A. A.; El-Sherbeeny, A. M.; Alhammadi, S.; Al Zoubi, W.; Ko, Y. G.; Abukhadra, M. R. Synthesis of Cellulose Fibers/Zeolite-A Nanocomposite as an Environmental Adsorbent for Organic and Inorganic Selenium Ions; Characterization and Advanced Equilibrium Studies. *J. Mol. Liq.* **2022**, *360*, 119573.
(56) Abukhadra, M. R.; Dardir, F. M.; Shaban, M.; Ahmed, E. A.; Soliman, M. F. Superior Removal of Co2+, Cu2+ and Zn2+ Contaminants from Water Utilizing Spongy Ni/Fe Carbonate-Fluorapatite; Preparation, Application and Mechanism. *Ecotoxicol. Environ. Saf.* **2018**, *157*, 358−368.
(57) Shaban, M.; Abukhadra, M. R.; Shahien, M. G.; Khan, A. A. P. Upgraded Modified Forms of Bituminous Coal for the Removal of Safranin-T Dye from Aqueous Solution. *Environ. Sci. Pollut. Res.* **2017**, *24* (22), 18135−18151.
(58) Dawodu, F. A.; Akpomie, G.; Abuh, M. Equilibrium Isotherm Studies on the Batch Sorption of Copper (II) Ions from Aqueous Solution unto Nsu Clay. *Int. J. Sci. Eng. Res.* **2012**, *3* (12), 1−7.
(59) Mobarak, M.; Ali, R. A. M.; Seliem, M. K. Chitosan/Activated Coal Composite as an Effective Adsorbent for Mn(VII): Modeling and Interpretation of Physicochemical Parameters. *Int. J. Biol. Macromol.* **2021**, *186*, 750−758.
(60) Dhaouadi, F.; Sellaoui, L.; Reynel-Ávila, H. E.; Landín-Sandoval, V.; Mendoza-Castillo, D. I.; Jaime-Leal, J. E.; Lima, E. C.; Bonilla-Petriciolet, A.; Lamine, A. B. Adsorption Mechanism of Zn2+, Ni2+, Cd2+, and Cu2+ Ions by Carbon-Based Adsorbents: Interpretation of the Adsorption Isotherms via Physical Modelling. *Environ. Sci. Pollut. Res.* **2021**, *28* (24), 30943−30954.
(61) Dhaouadi, F.; Sellaoui, L.; Badawi, M.; Reynel-Ávila, H. E.; Mendoza-Castillo, D. I.; Jaime-Leal, J. E.; Bonilla-Petriciolet, A.; Lamine, A. B. Statistical Physics Interpretation of the Adsorption Mechanism of Pb2+, Cd2+ and Ni2+ on Chicken Feathers. *J. Mol. Liq.* **2020**, *319*, 114168.
(62) Ali, R. A. M.; Mobarak, M.; Badawy, A. M.; Lima, E. C.; Seliem, M. K.; Ramadan, H. S. New Insights into the Surface Oxidation Role in Enhancing Congo Red Dye Uptake by Egyptian Ilmenite Ore: Experiments and Physicochemical Interpretations. *Surf. Interfaces* **2021**, *26*, 101316.
(63) Sellaoui, L.; Ali, J.; Badawi, M.; Bonilla-Petriciolet, A.; Chen, Z. Understanding the Adsorption Mechanism of Ag+ and Hg2+ on Functionalized Layered Double Hydroxide via Statistical Physics Modeling. *Appl. Clay Sci.* **2020**, *198*, 105828.
(64) Sellaoui, L.; Guedidi, H.; SarraWjihi, S.; Reinert, L.; Knani, S.; Duclaux, L.; Ben Lamine, A. Experimental and Theoretical Studies of Adsorption of Ibuprofen on Raw and Two Chemically Modified Activated Carbons: New Physicochemical Interpretations. *RSC Adv.* **2016**, *6* (15), 12363−12373.
(65) Pashai Gatabi, M.; Milani Moghaddam, H.; Ghorbani, M. Efficient Removal of Cadmium Using Magnetic Multiwalled Carbon Nanotube Nanoadsorbents: Equilibrium, Kinetic, and Thermodynamic Study. *J. Nanopart. Res.* **2016**, *18* (7), 189.
(66) Anbia, M.; Kargosha, K.; Khoshbooei, S. Heavy Metal Ions Removal from Aqueous Media by Modified Magnetic Mesoporous Silica MCM-48. *Chem. Eng. Res. Des.* **2015**, *93*, 779−788.
(67) Kenawy, I. M. M.; Abou El-Reash, Y. G.; Hassanien, M. M.; Alnagar, N. R.; Mortada, W. I. Use of Microwave Irradiation for Modification of Mesoporous Silica Nanoparticles by Thioglycolic Acid for Removal of Cadmium and Mercury. *Microporous Mesoporous Mater.* **2018**, *258*, 217−227.
(68) Aguado, J.; Arsuaga, J. M.; Arencibia, A.; Lindo, M.; Gascón, V. Aqueous Heavy Metals Removal by Adsorption on Amine-Functionalized Mesoporous Silica. *J. Hazard. Mater.* **2009**, *163* (1), 213−221.
(69) Feng, G.; Ma, J.; Zhang, X.; Zhang, Q.; Xiao, Y.; Ma, Q.; Wang, S. Magnetic Natural Composite Fe3O4-Chitosan@bentonite for Removal of Heavy Metals from Acid Mine Drainage. *J. Colloid Interface Sci.* **2019**, *538*, 132−141.
(70) Li, Z.; Wang, L.; Meng, J.; Liu, X.; Xu, J.; Wang, F.; Brookes, P. Zeolite-Supported Nanoscale Zero-Valent Iron: New Findings on Simultaneous Adsorption of Cd(II), Pb(II), and As(III) in Aqueous Solution and Soil. *J. Hazard. Mater.* **2018**, *344*, 1−11.
(71) Bian, Y.; Bian, Z.-Y.; Zhang, J.-X.; Ding, A.-Z.; Liu, S.-L.; Wang, H. Effect of the Oxygen-Containing Functional Group of Graphene Oxide on the Aqueous Cadmium Ions Removal. *Appl. Surf. Sci.* **2015**, *329*, 269−275.
(72) Luo, C.; Wei, R.; Guo, D.; Zhang, S.; Yan, S. Adsorption Behavior of MnO2 Functionalized Multi-Walled Carbon Nanotubes for the Removal of Cadmium from Aqueous Solutions. *Chem. Eng. J.* **2013**, *225*, 406−415.
(73) Tofighy, M. A.; Mohammadi, T. Adsorption of Divalent Heavy Metal Ions from Water Using Carbon Nanotube Sheets. *J. Hazard. Mater.* **2011**, *185* (1), 140−147.
(74) Chen, J.; Fang, K.; Wu, L.; Qian, Z.; Chen, J. Removal of Cd(II) from Aqueous by Adsorption onto Mesoporous Ti-MCM-48. *Procedia Environ. Sci.* **2011**, *10*, 2491−2497.
(75) Cui, X.; Fang, S.; Yao, Y.; Li, T.; Ni, Q.; Yang, X.; He, Z. Potential Mechanisms of Cadmium Removal from Aqueous Solution by Canna Indica Derived Biochar. *Sci. Total Environ.* **2016**, *562*, 517−525.
(76) Madala, S.; Nadavala, S. K.; Vudagandla, S.; Boddu, V. M.; Abburi, K. Equilibrium, Kinetics and Thermodynamics of Cadmium (II) Biosorption on to Composite Chitosan Biosorbent. *Arab. J. Chem.* **2017**, *10*, S1883−S1893.

https://doi.org/10.1021/acsomega.3c08592
ACS Omega 2024, 9, 11534−11550

(77) Zheng, S.; Xia, S.; Han, S.; Yao, F.; Zhao, H.; Huang, M. β-Cyclodextrin-loaded minerals as novel sorbents for enhanced adsorption of Cd2+ and Pb2+ from aqueous solutions. *Sci. Total Environ.* **2019**, *693*, 133676.
(78) Jiang, M.; Chen, L.; Niu, N. Enhanced Adsorption for Malachite Green by Functionalized Lignin Magnetic Composites: Optimization, Performance and Adsorption Mechanism. *J. Mol. Struct.* **2022**, *1260*, 132842.
(79) Wang, Y.; Zhou, R.; Wang, C.; Zhou, G.; Hua, C.; Cao, Y.; Song, Z. Novel Environmental-Friendly Nano-Composite Magnetic Attapulgite Functionalized by Chitosan and EDTA for Cadmium (II) Removal. *J. Alloys Compd.* **2020**, *817*, 153286.
(80) Obregón-Valencia, D.; Sun-Kou, M. d. R. Comparative Cadmium Adsorption Study on Activated Carbon Prepared from Aguaje (Mauritia Flexuosa) and Olive Fruit Stones (Olea Europaea L.). *J. Environ. Chem. Eng.* **2014**, *2* (4), 2280−2288.
(81) Chen, L.; Wu, P.; Chen, M.; Lai, X.; Ahmed, Z.; Zhu, N.; Dang, Z.; Bi, Y.; Liu, T. Preparation and Characterization of the Eco-Friendly Chitosan/Vermiculite Biocomposite with Excellent Removal Capacity for Cadmium and Lead. *Appl. Clay Sci.* **2018**, *159*, 74−82.
(82) Monier, M.; Abdel-Latif, D. A. Preparation of Cross-Linked Magnetic Chitosan-Phenylthiourea Resin for Adsorption of Hg(II), Cd(II) and Zn(II) Ions from Aqueous Solutions. *J. Hazard. Mater.* **2012**, *209−210*, 240−249.

https://doi.org/10.1021/acsomega.3c08592
ACS Omega 2024, 9, 11534−11550